TNO Built Environment and Geosciences

Laan van Westenenk 501
P.O. Box 342
7300 AH Apeldoorn
The Netherlands

www.tno.nl

P +31 55 549 34 93
F +31 55 541 98 37

TNO-report

90-346

Instantaneous and continuous release tests for intercomparison of experimental equipment

Date	October 1990
Authors	H. van Oort P.J.H. Builtjes
Order no.	8724-21050
Keywords	- dispersion - heavy gas - wind tunnel measurements
ST-code	G8
	Activities carried out within the framework of the CEC research programme on Major Technological Hazards, project BA 'Research on continuous and instantaneous heavy gas clouds'
Intended for	Commission of the European Communities Directorate – General for Science, Research and Development XII/G 200, Rue de la Loi B-1049 Brussels Belgium

SUMMARY

Two experiments, an instantaneous and a continuous release test, have been carried out and reported.
The results will be used to intercompare with the results of identical experiments, carried out by Warren Spring Laboratory (UK) and the University of Hamburg (FRG).
These experiments are carried out in the framework of the CEC, research programme on Major Technological Hazards, project BA 'research on continuous and instantaneous heavy gas clouds'.
Additional tests varying the wind speed are also reported.

TABLE OF CONTENTS

1. INTRODUCTION

During the joint CEC-project BA 'research on continuous and instantaneous heavy gas clouds', which is part of the Major Technological Hazards Program, wind tunnel experiments on heavy gas dispersion, investigating both mean and fluctuating concentrations, have been carried out at three institutes, viz. Warren Spring Laboraty (UK), University of Hamburg (FRG) and MT-TNO (NL). It should be guaranteed that the experimental equipment used by the three institutes will measure the same mean and fluctuating concentrations under identical circumstances. In this way different experiments performed in one of the three wind tunnels can be considered as to belong to one coherent experimental data base. Consequently, a comparison has been made between the equipment used including the test facilities. The two experiments carried out at MT-TNO for the intercomparison are described in this report. The description of both tests are given by Schatzmann [1].

The atmospheric boundary layer wind tunnel used in the MT-TNO experiments is described in section 2. The fast aspirated hot wire probe for measuring concentration fluctuations is described in section 3. In section 4 the instantaneous release experiments (one of both tests) are described, while in section 5 the continuous release experiments are described.

2. WIND TUNNEL

In figure 1 a schematic drawing of the PIA (Pollution Industrial Aerodynamics) wind tunnel is given.
The test section of the PIA wind tunnel has a cross section of 2.65 * 1.2 m^2, and a length in normal circumstances of 6.8 m. The wind speed in the test section can be set between about 0.2 m/s and 20 m/s. The boundary layer simulation method used in the wind tunnel is the method developed by Counihan, and is described in detail by Builtjes and Vermeulen [2].
The atmospheric boundary layer in both experiments was simulated by using a smooth carpet, resulting in a roughness length scale z_o of about 0.05 mm. In figure 2 the profiles of the mean velocity and the along wind turbulence are drawn for a reference velocity close to that used in the experiments.
Figure 3 shows that the logarithmic velocity profile, based on the above mentioned roughness length scale, fits well with the exponential velocity profile with exponent n=0.16 (which has been used in the wind tunnel of the University of Hamburg) in the region from 0.01 to 1.0 m. heigth, which is just the region in which the mixing process takes place (the z_o-values in figure 3 are available in the PIA wind tunnel).
For a detailed description of the velocity profiles and the turbulence intensities at different surface roughnesses the reader is referred to Builtjes and Vermeulen [2].

3. ASPIRATED HOT WIRE PROBE

The principle of the aspirated hot wire probe is based on the fact that the heat transfer from a thin heated cylinder in a gas depends on the flow speed and the physical properties of the gas. In an aspirated probe, the flow rate is kept constant, so that a variation of the physical properties of the gas, due to a concentration change, will lead to a change in heat transfer. The problem, however, is that it is difficult to obtain a flow rate, which is constant in time with a high precision, because the flow rate in reality always depends in some way on the pressure drop in the probe system, which in turn depends on the physical properties of the gas mixture too. In the MT-TNO probe this problem is solved by applying a sonic nozzle. The flow rate is then independent of the pressure drop over the nozzle. The hot wire should be positioned just before the sonic nozzle, because the suction velocity depends on the sonic speed, which on its turn depends on the composition of the gasmixture. In the MT-TNO probe the hot wire is positioned 1.5 mm before the sonic nozzle.

A schematic drawing of the MT-TNO probe, used in the intercomparison tests, is given in figure 4a. The intake diameter is 2 mm. and the suction velocity is about .5 m/s (for air), which results in a suction rate of 5.6 l/h. When using SF6 the suction velocity amounts .2 m/s, resulting in a suction rate of 2.2 l/h. The frequency response of this probe appeared to be about 70 Hz. when using SF6 (-3dB point).
This probe sometimes shows a zero drift, of which the cause is not clear. Therefore, the MT-TNO probe has recently been modified. This modified probe is drawn in figure 4b. This probe differs from the previous probe in both the geometry and the type of hot wire. Moreover, the hot wire is placed parallel to the flow (in the previous probe the hot wire was placed perpendicular to the flow). Due to the new type of hot wire and the changed orientation of the wire the modified probe appears to have a smaller zero drift. Due to the new, smaller geometry of the probe, the flow disturbance has also been decreased. The modified probe has an intake diameter of 2.2 mm. and the suction velocity is about 1.2 m/s (for air), resulting in a suction rate of 16 l/h. For SF6 the suc-

tion velocity amounts 0.5 m/s, resulting in a suction rate of 6.4 l/h. The frequency response amounts about 70 Hz. for SF_6. In addition this probe has the advantage that it is easier to calibrate and to repair. All experiments reported here are performed with the old probe (fig. 4a).

4. INSTANTANEOUS RELEASE

The instantaneous release experiment is a modelling of Thorney Island Trial No. 17.

The full scale release conditions are:

Released gas volume	:	$V0$	= 1700 m³
Initial density excess	:	$(\rho o - \rho a)/\rho a$	= 3.2
Characteristic length	:	Lci	= 11.9 m
Characteristic velocity	:	Uci	= 19.4 m/s
Characteristic time	:	Tci	= 0.6 s
Ambient wind	:	Ur	= 0.26 Uci (at 0.84 Lci)

The model release conditions are:

Released gas volume	:	$V0$	= $1.4 * 10^{-3}$ m³ (model scale 1:107)
Initial density excess	:	$(\rho o - \rho a)/\rho a$	= 4.12 (SF_6)
Characteristic length	:	Lci	= 0.112 m
Characteristic velocity	:	Uci	= 2.126 m/s
Characteristic time	:	Tci	= 0.053 s
Wind speed	:	Ur	= 0.26 Uci (at 0.84 Lci)

The sampling rate is 60 Hz.
The atmospheric boundary layer was modelled as described in section 2.
One probe has been used for the measurements.

The release device consist of a cilindrical tube of .13 m. diameter and a height of .105 m. (figure 5). This tube is retractable in the floor of the wind tunnel. The top of the tube is closed with a lid which is removed just before each experiment by simply pulling a string. Seven sampling stations have been used, with the following coordinates (figure 6):

sampling station [no.]	x-coordinate [Lci]	y-coordinate [Lci]	z-coordinate [Lci]
1	1.87	1.68	0.034
2	3.12	2.79	0.034
3	4.37	3.92	0.034
4	5.61	5.04	0.034
5	5.91	-0.33	0.034
6	8.88	-0.48	0.034
7	11.84	-0.64	0.034

coordinates: x - downstream
y - lateral
z - height | origin in the middle of the gas source, at the wind tunnel floor

The experimental results are given in figure 7 (sampling station 1 and 2) to figure 10 (sampling station 7).

In figure 11a and 11b the measured maximum concentrations are given as function of the dimensionless distance to the source R/Lcc. The pictures clearly show the decrease of maximum concentration with increasing distance from the source, due to the dispersion of the gas. Continuous release experiments, carried out by Hall [3], show a large influence of the ground roughness on the downward concentration. Recent comparable experiments, carried out by MT-TNO (not yet published) confirm this effect. This means that for the interpretation of the intercomparison tests, the ground roughness must be taken into account.

The arrival times of the gas cloud at the different stations can not be get from the pictures, because the zero-time values (T/Tci=0) have not been determined accurately enough for a detailed analysis.

5. CONTINUOUS RELEASE

The model release conditions are:

Gas release rate	:	$\dot{V}0$	= 1.744 * 10^{-4} m³/s (628 l/h)
Initial density excess	:	$(\rho o - \rho a)/\rho a$	= 4.12 (SF6)
Characteristic length	:	Lcc	= 0.015 m
Characteristic velocity	:	Ucc	= 0.779 m/s
Characteristic time	:	Tcc	= 0.019 s
Wind speed	:	Ur	= 1.0 Ucc (at 1.0 Lcc)

The sampling rate is 60 Hz.
The atmospheric boundary layer was modelled as described in section 2. One probe has been used for the measurements. This probe was mounted with the tip on the surface at different sampling stations (described below), see figure 5.

The release source is circular, .107 m diameter and flat with the wind tunnel floor. The source is covered with a gaze of 50% porosity. The outflow velocity of the gas amounts v_{out} = 0.0388 m/s (= 0.05 Ucc). Eight sampling stations have been used, with the following coordinates (figure 12):

sampling station [no.]	x-coordinate [Lci]	y-coordinate [Lci]	z-coordinate [Lci]
1	42.7	0.0	0.0
2	85.5	0.0	0.0
3	128.2	0.0	0.0
4	171.0	0.0	0.0
5	213.7	0.0	0.0
6	256.4	0.0	0.0
7	299.5	0.0	0.0
8	342.3	0.0	0.0

coordinates: x - downstream
y - lateral
z - height

origin in the middle of the gas source, at the wind tunnel floor

The experimental results are given in figure 13 to figure 20. At most locations repeated measurements have been carried out and are inserted in the figures.

In figure 25 the measured mean, minimum and maximum concentrations are given as function of the dimensionless distance downwind from the source, X/Lcc (averaging time from T/Tcc=0 to T/Tcc=5263). The picture shows clearly the decrease of gas concentration with increasing distance to the source. The concentrations at sample station 5 are relatively low; moreover, the minimum value of measured concentration is below zero (-0.5%). This may be due to zero drift, mentioned in chapter 3, of which the reason is not clear. The same effect may have occurred at sample station 7 and 8. In figure 26 the standard deviation is given as function of the dimensionless downward distance, which shows a decrease of the standard deviation with increasing distance.
Recently, continuous release experiments have been carried out at different ground roughnesses, which show a large influence of the ground roughness on the downward concentrations (see also chapter 4). These experiments will be reported.

Besides the above experiments, two additional continuous release tests have been carried out, which do not belong to the intercomparison. Both tests however are interesting with relation to gas dispersion. The experimental set-up in both tests is equal to that described above, except the wind speed: in the first additional test the wind speed is 0.5 Ucc at 1.0 Lcc height; in the second test the wind speed is 2.0 Ucc at 1.0 Lcc height. The experimented results are given in figure 21 to figure 24. The summarized results are given in figure 27 (mean concentration) and 28 (standard deviation). From figure 27 it can be seen that the wind speed has a large effect on the downward gas concentration: a higher wind speed leads to a lower gas concentration at a fixed downward spot. The influence of the wind speed on the standard deviation (figure 28) is less clear.

6. CONCLUSIONS

Two intercomparison tests have been carried out and reported. The results will be used to intercompare with the results of identical experiments, carried out by the University of Hamburg (FRG), described in [1], and by Warren Spring Laboratory (UK), described in [3].
Recent experiments carried out by Hall [3] and MT-TNO [not yet reported] show a large influence of the ground roughness on the downward gas concentration. This means that ground roughness, used in the experiments, have to be involved in the analysis of the intercomparison tests.

Additional tests show the influence of the wind speed on the downward gas concentration: an increasing wind speed leads to a decrease of the gas concentration.

7. REFERENCES

[1] Schatzmann, M
Intercomparison of wind tunnels
First progress report of project BA (topic 1.2)
'Research on continuous and instantaneous heavy gas clouds'
November 1, 1987 - June 1, 1988
(MT-TNO ref. nr. 88-09097/8724-18768)

[2] Builtjes, Peter; Vermeulen, Paul
Atmospheric boundary layer simulation in the PIA and MIA
wind tunnels of TNO-Apeldoorn.
MT-TNO ref. nr. 80-0290, January, 1980

[3] Hall, D.J., Marsland, G.A.; Emmot, M.A.
CEC-MTH wind tunnel intercomparison of heavy
gas dispersion
Warren Spring Laboratory
ref. nr. CR 3256 (PA)

8. AUTHENTICATION

- Name and address of the principal:

  MT-TNO
  P.O. Box 342
  7300 AH Apeldoorn
  The Netherlands

- Names and functions of the cooperators:

  A. de Wilde - technician
  H. van Oort - scientist

- Names of establishments to which part of the research was put out to contract:

- Date upon which, or period in which, the research took place:

  November 1, 1987 - October 1, 1990

- Signature:

	Approved by:
P.J.H. Builtjes	B. Stork
research coordinator	Head of department

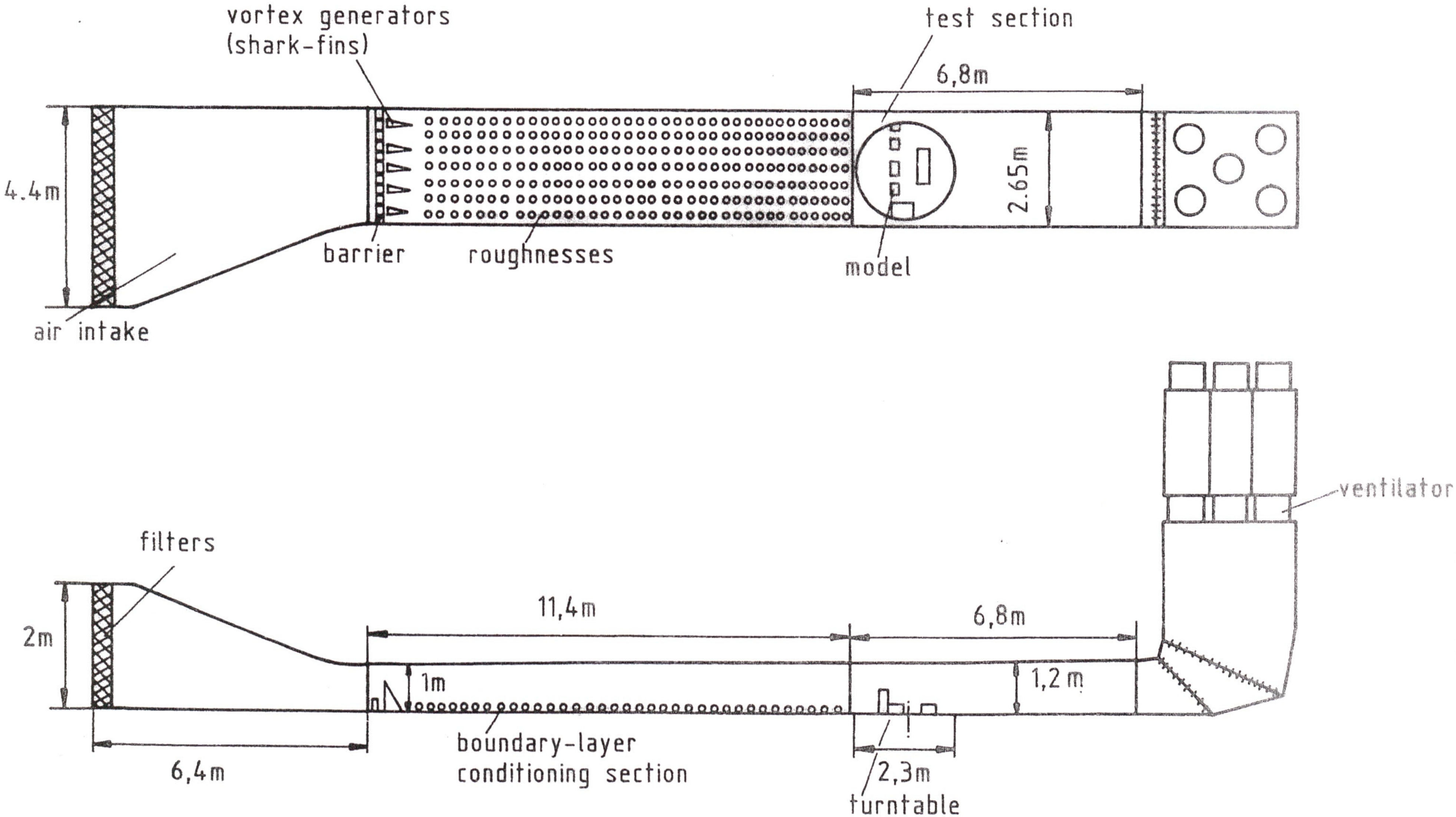

The PIA wind-tunnel.

MT-TNO
90-346
Fig. 1

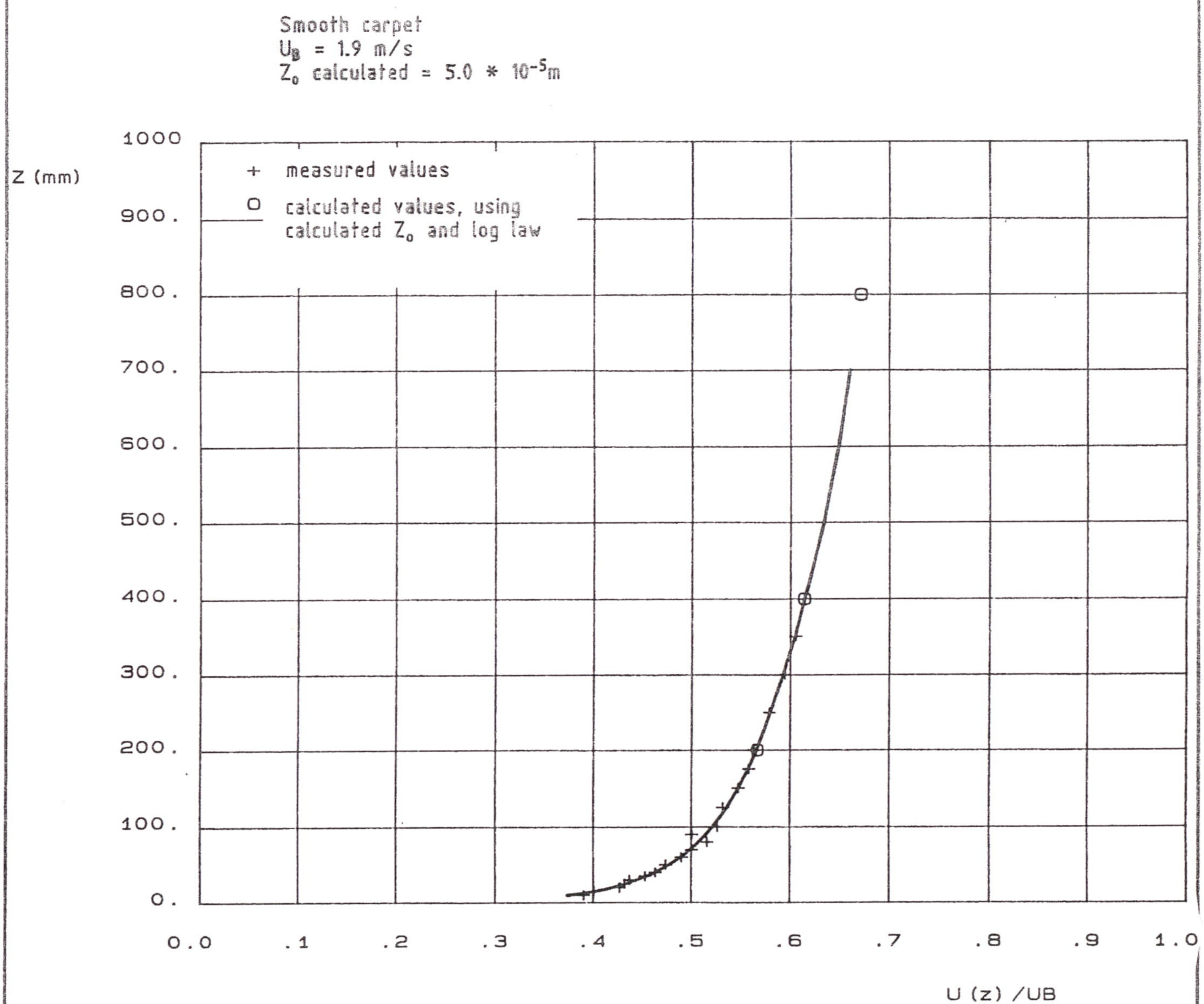

Mean velocity profile.	MT-TNO 90-346 Fig.2a

Smooth carpet

U_B = 1.9 m/s
Z_0 calculated = 5.0 * 10^{-5}m

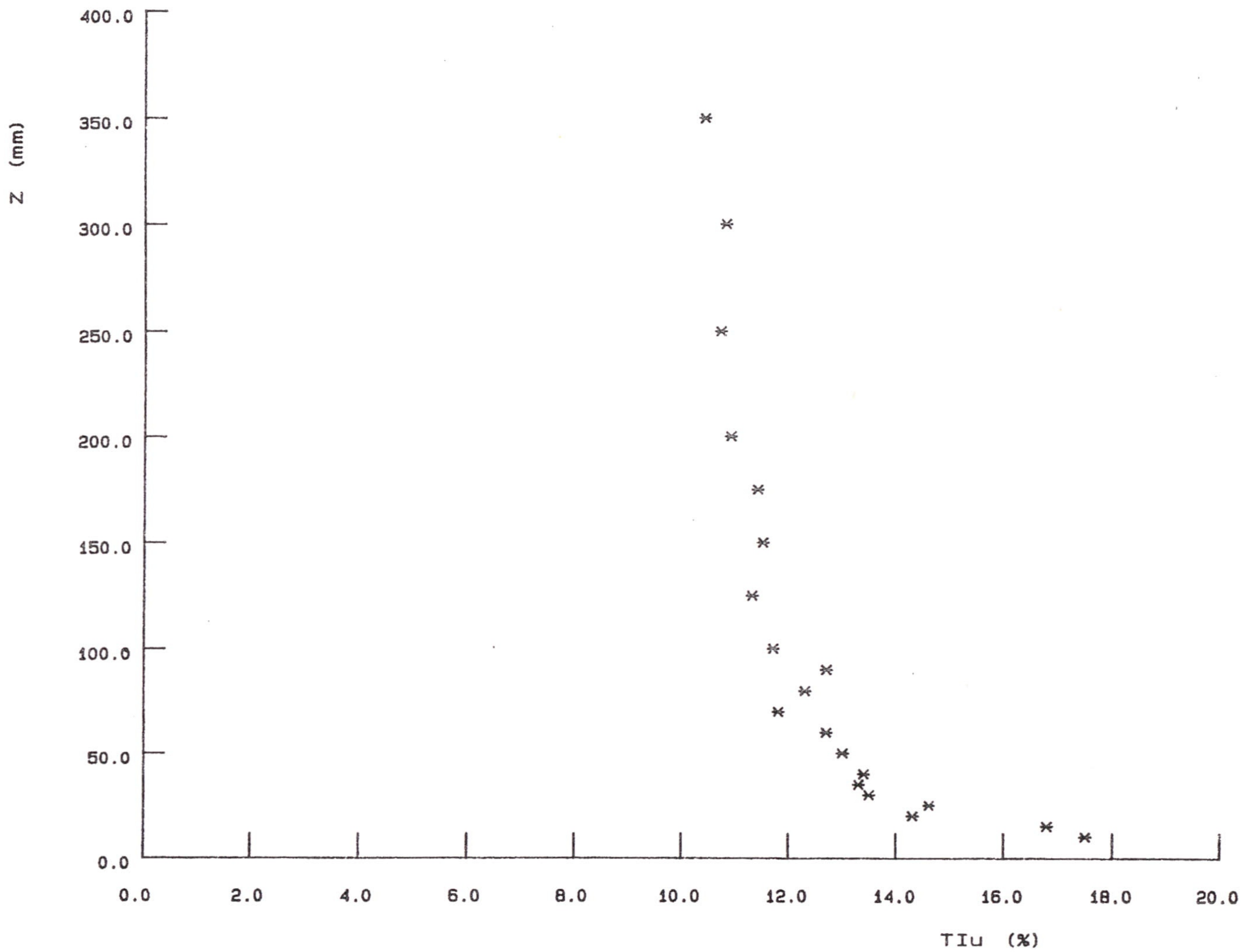

Longitudinal turbulence intensity profile.	MT-TNO 90-346 Fig.2b

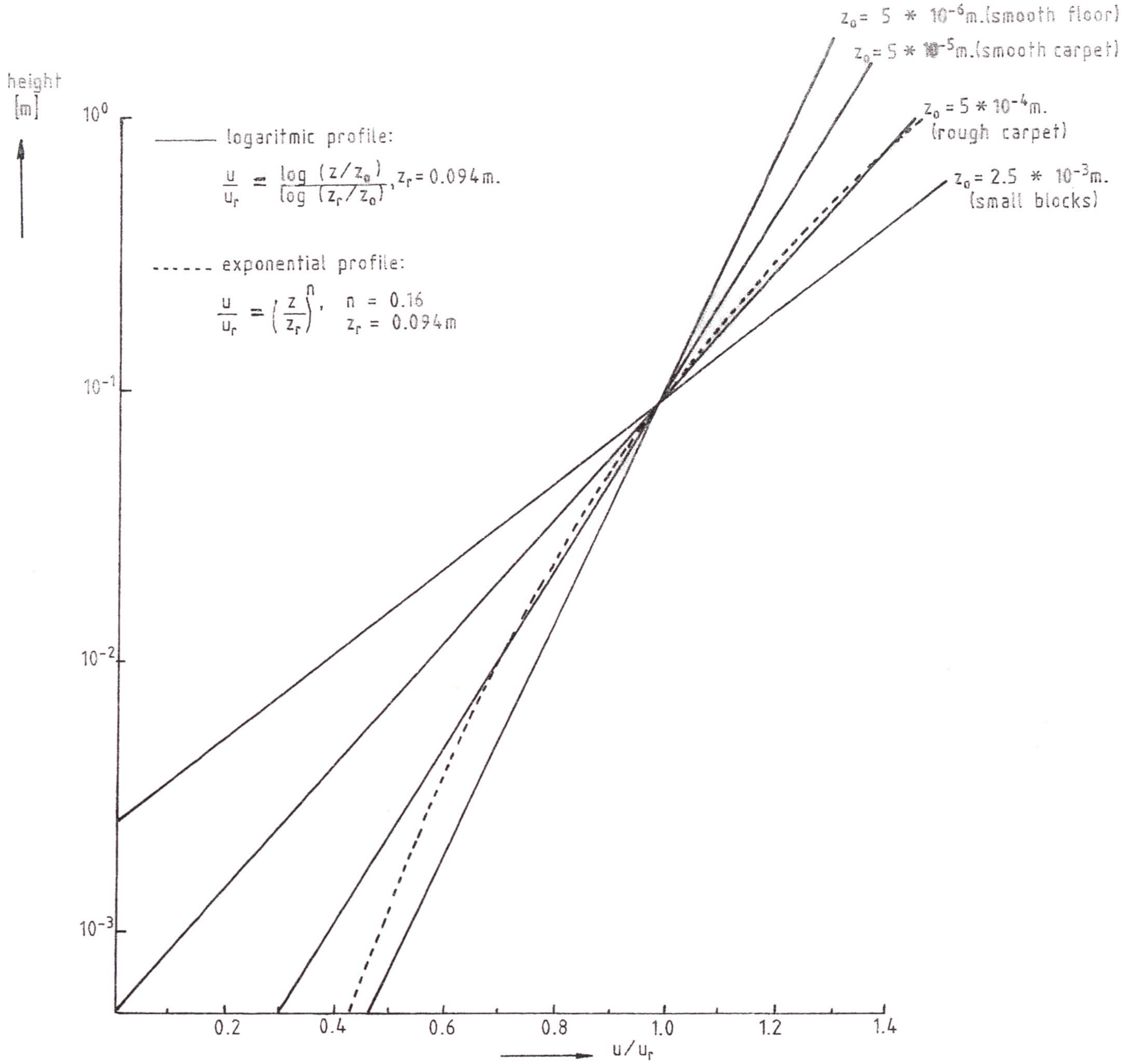

Comparison between logaritmic and exponential velocity profile.	MT-TNO 90-346 Fig.3

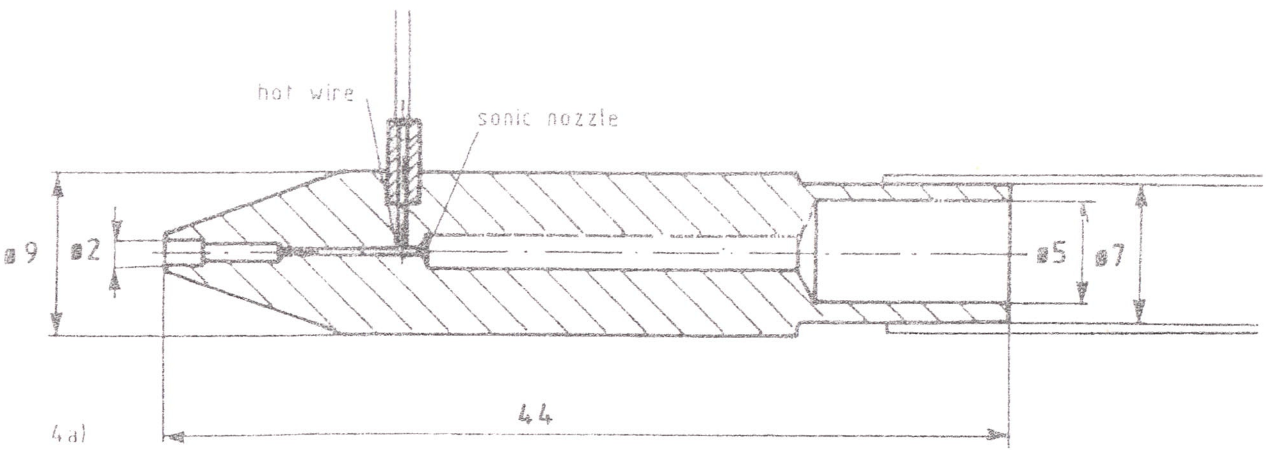

4a)

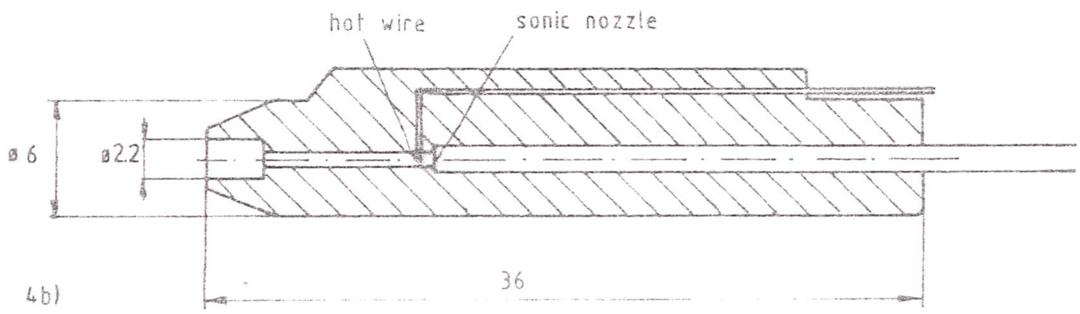

4b)

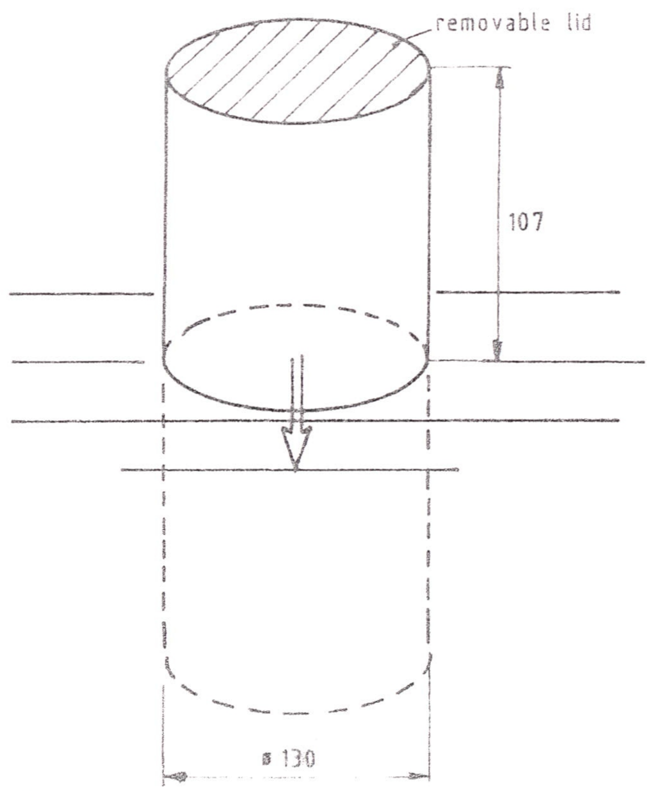

5)

(measures in mm)

4a) MT-TNO probe. 4b) Modified MT-TNO probe. 5) Release device in the instantaneous experiments..	MT-TNO 90-346 Fig.4a 4b & 5

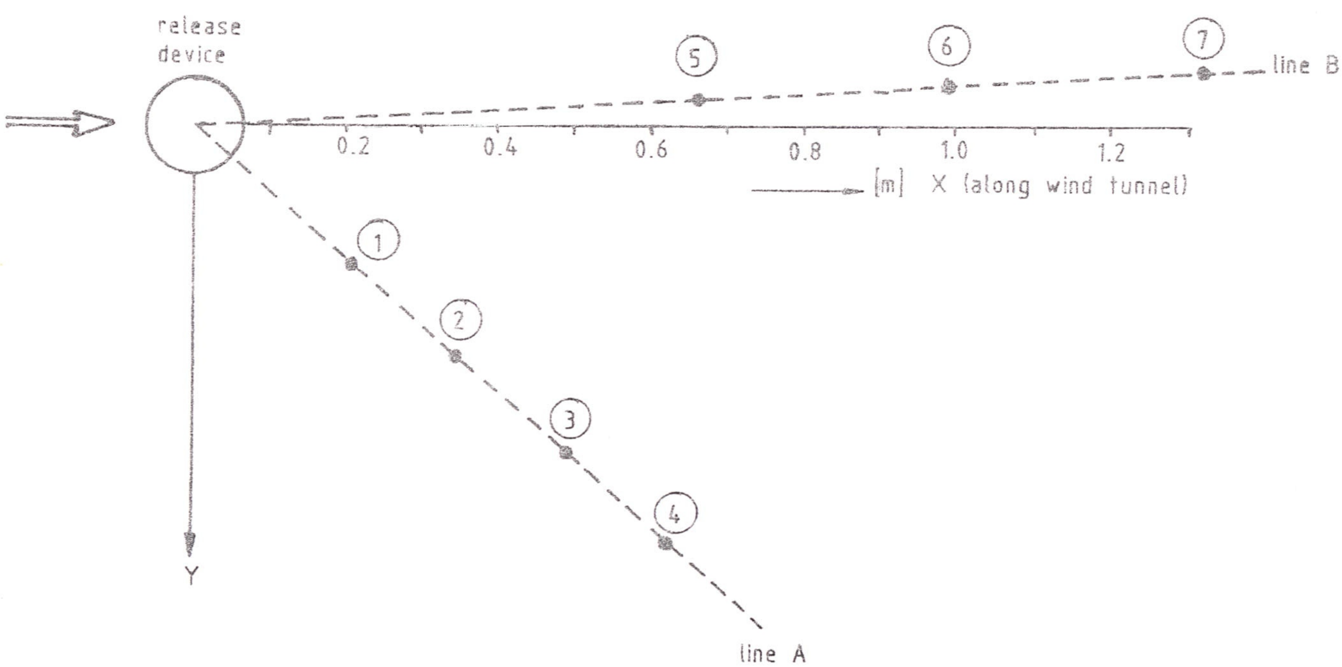

Sampling stations for the instantaneous test.

MT-TNO
90-346
Fig.6

Instantaneous Release

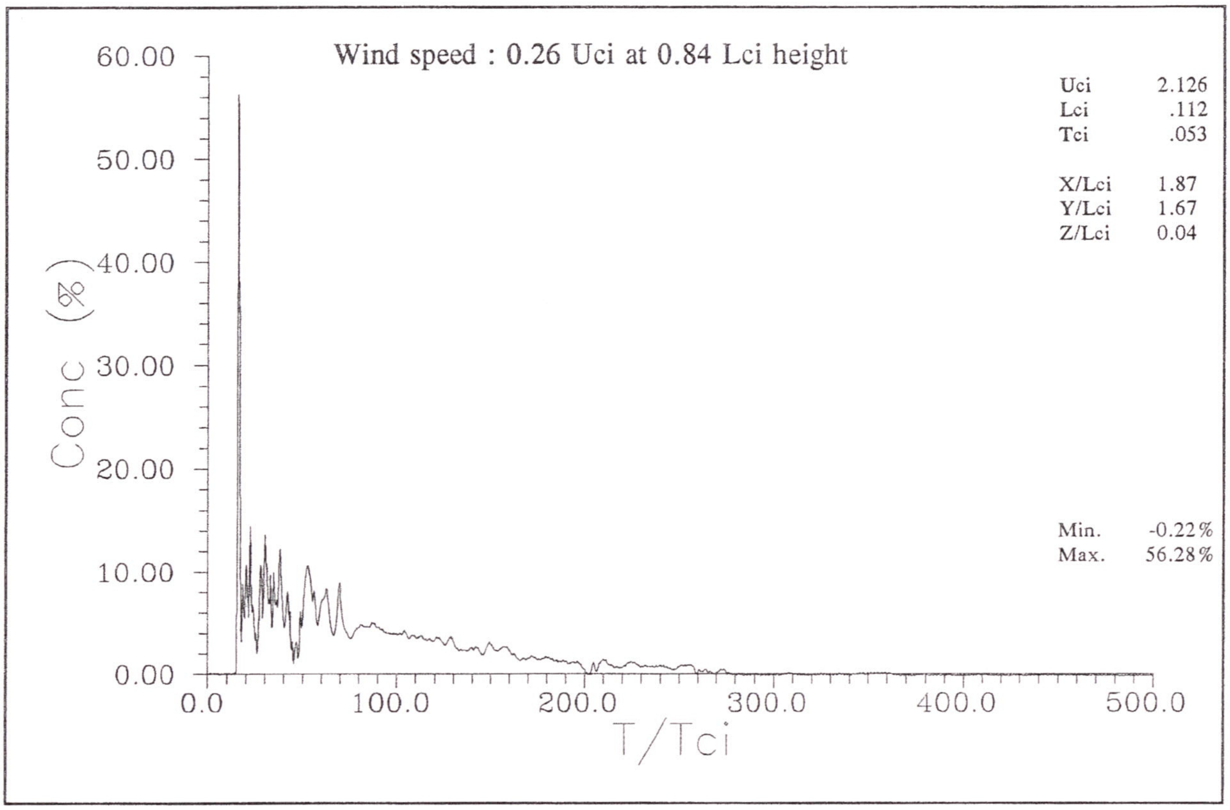

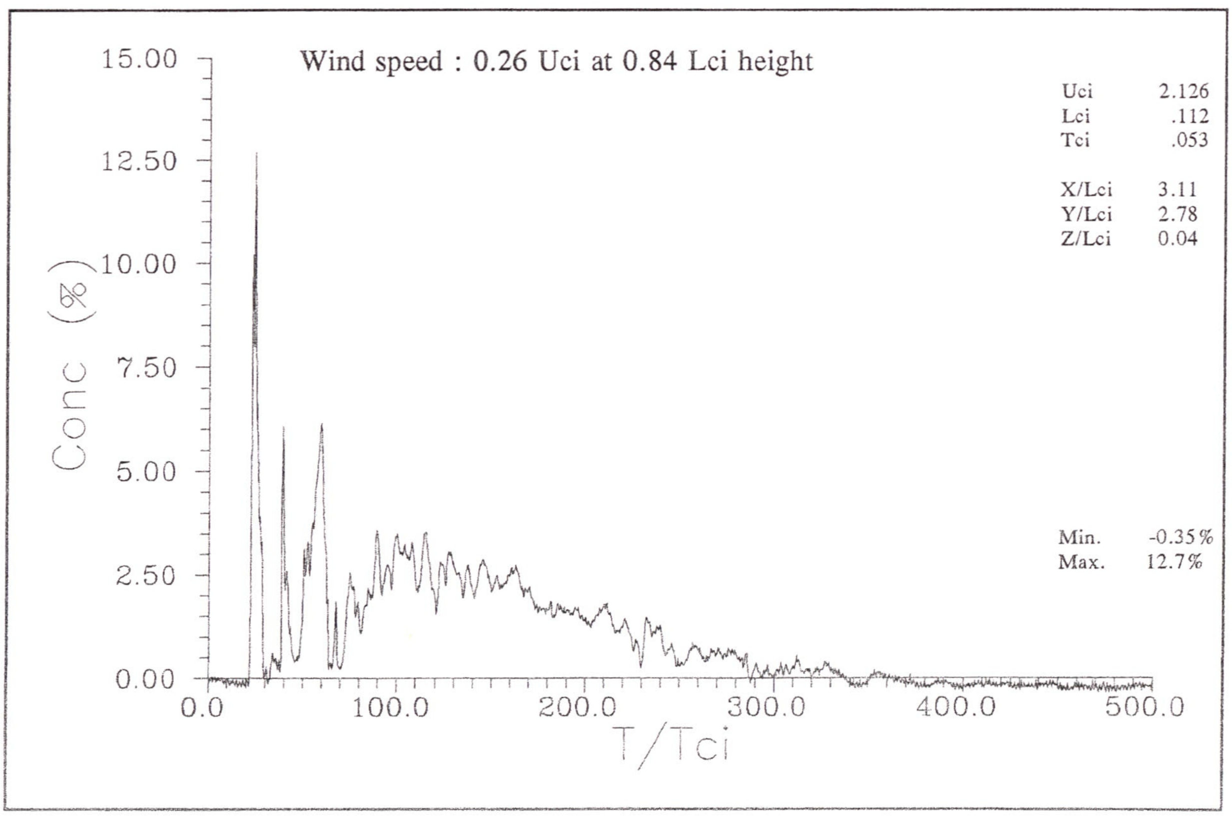

Figure 7 Results of the Instantaneous release .

Instantaneous Release

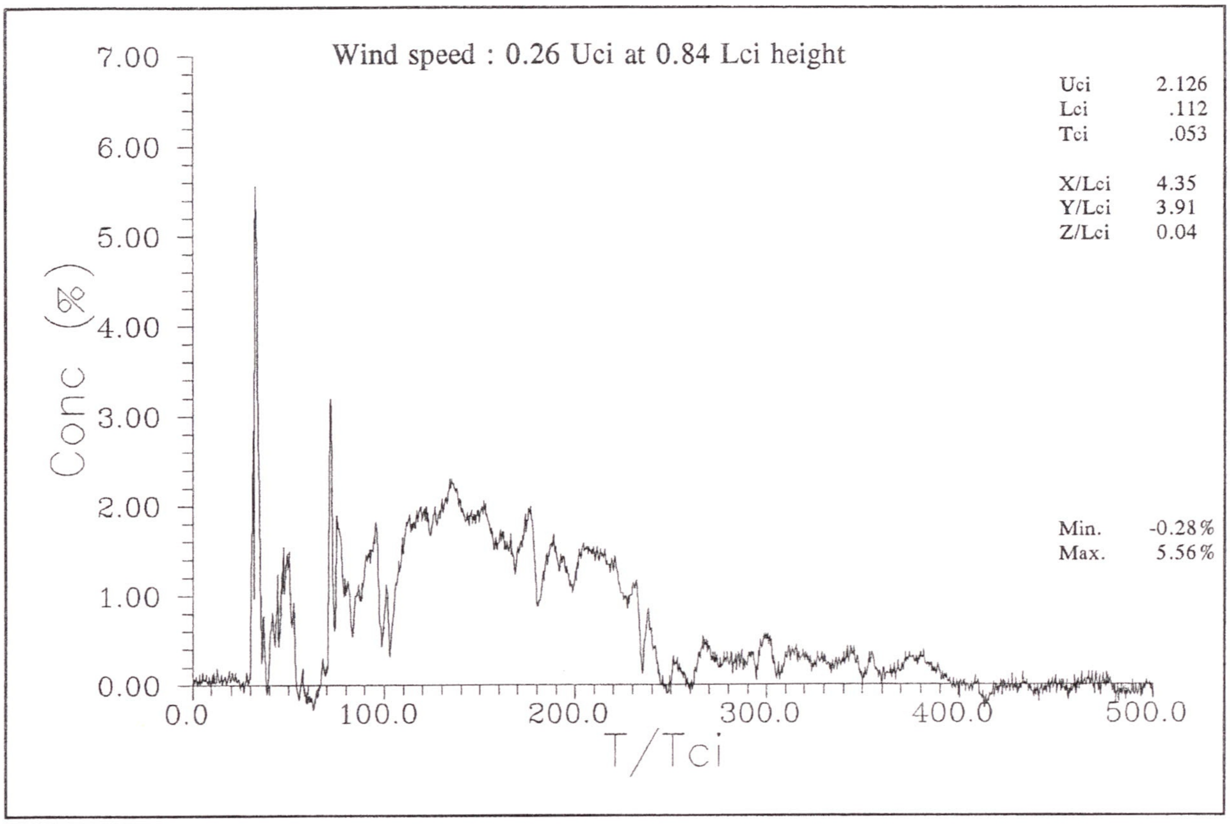

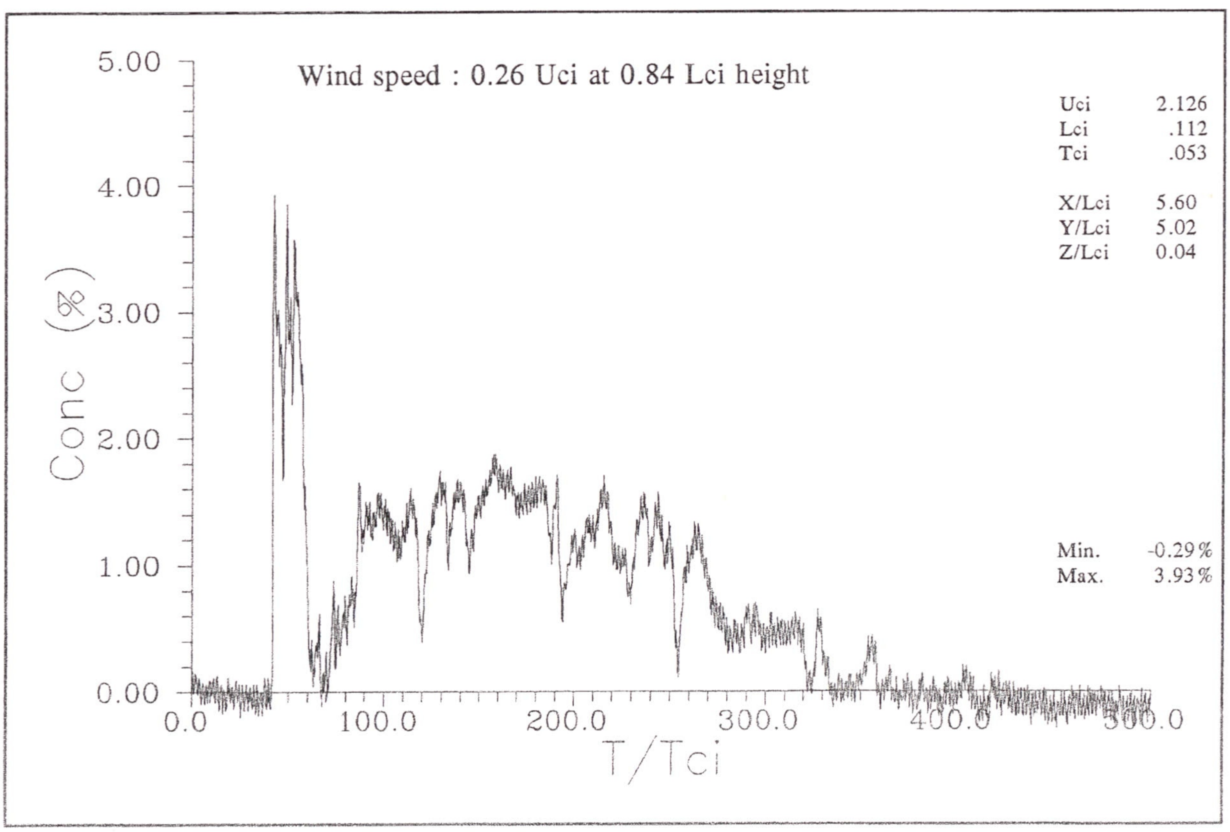

Figure 8 Results of the Instantaneous release .

Instantaneous Release

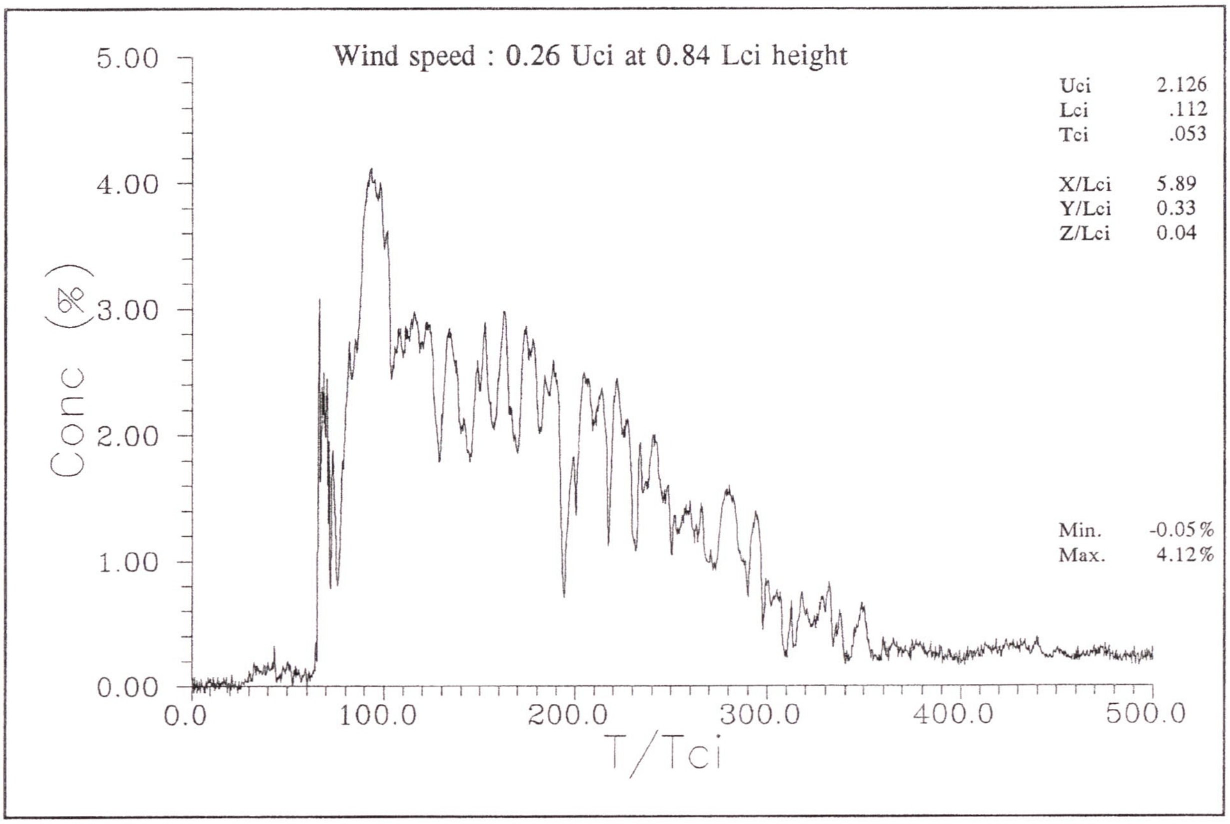

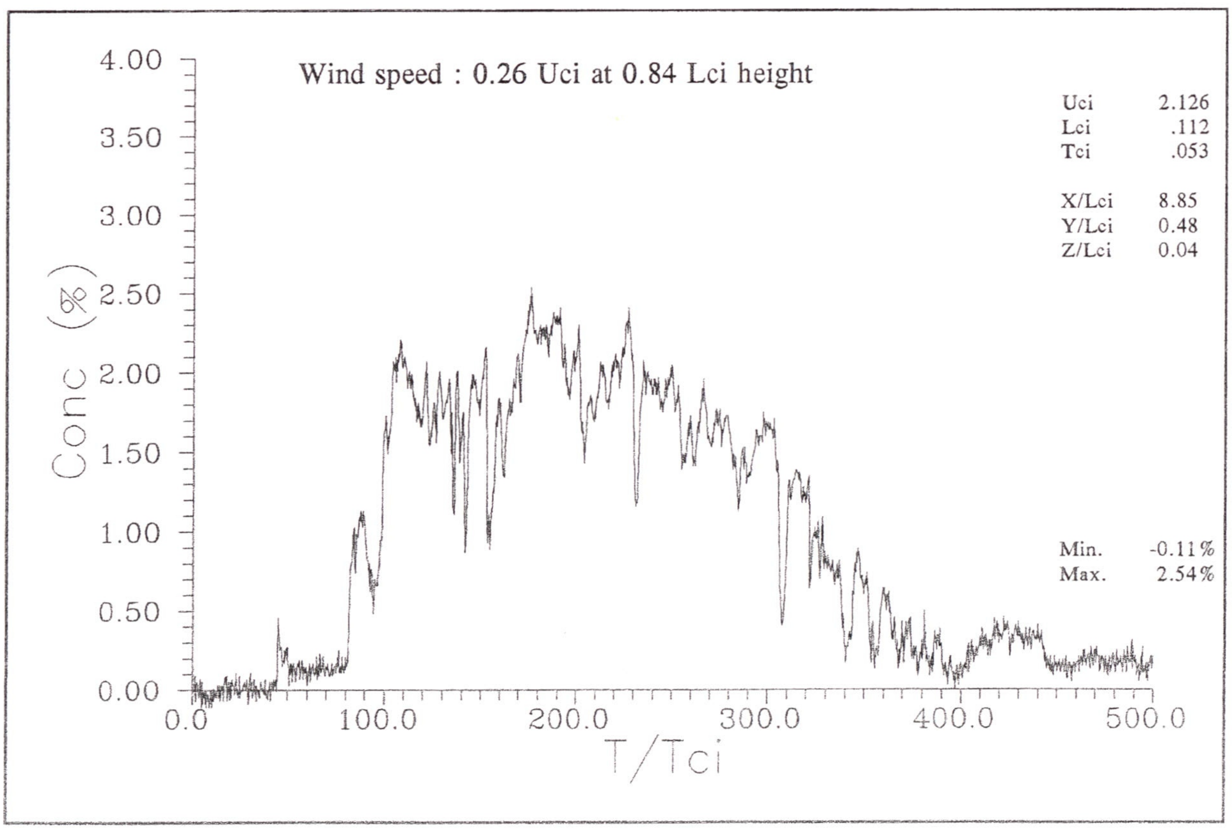

Figure 9 Results of the Instantaneous release .

Instantaneous Release

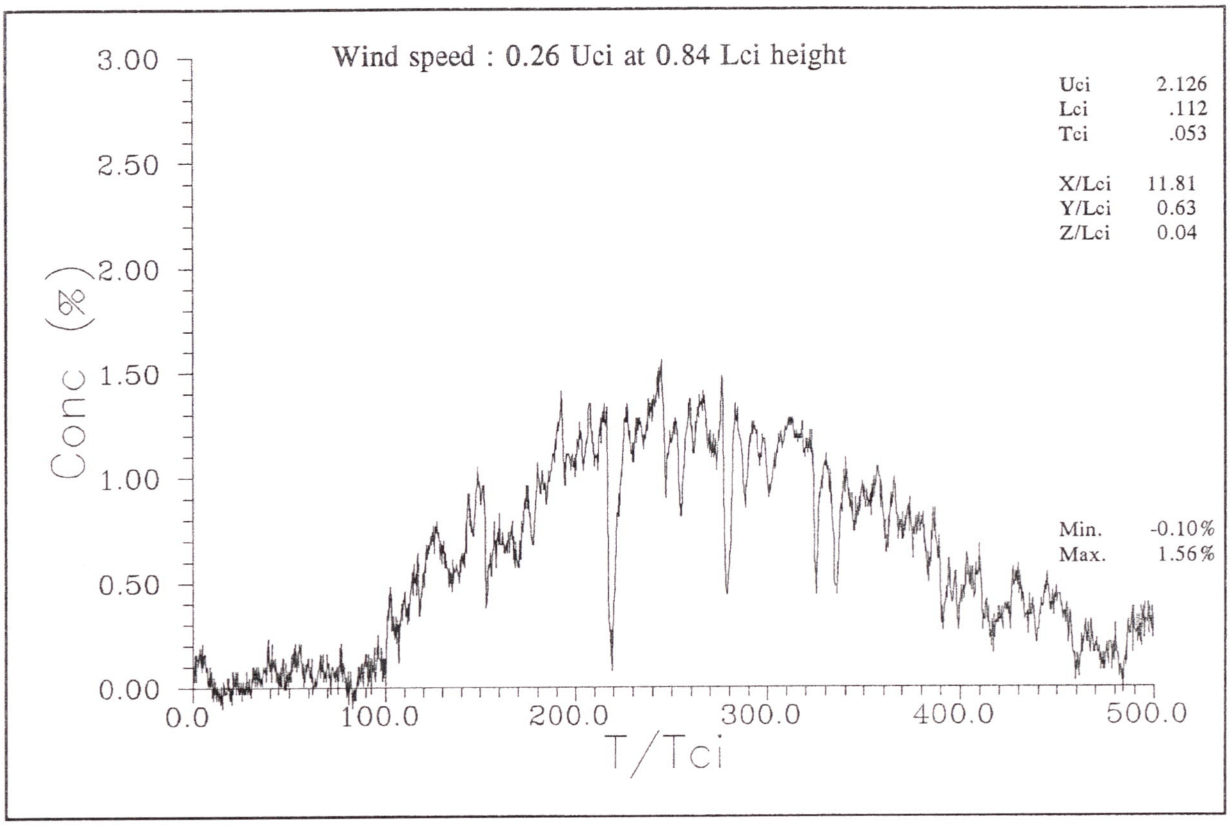

Figure 10 Results of the Instantaneous release .

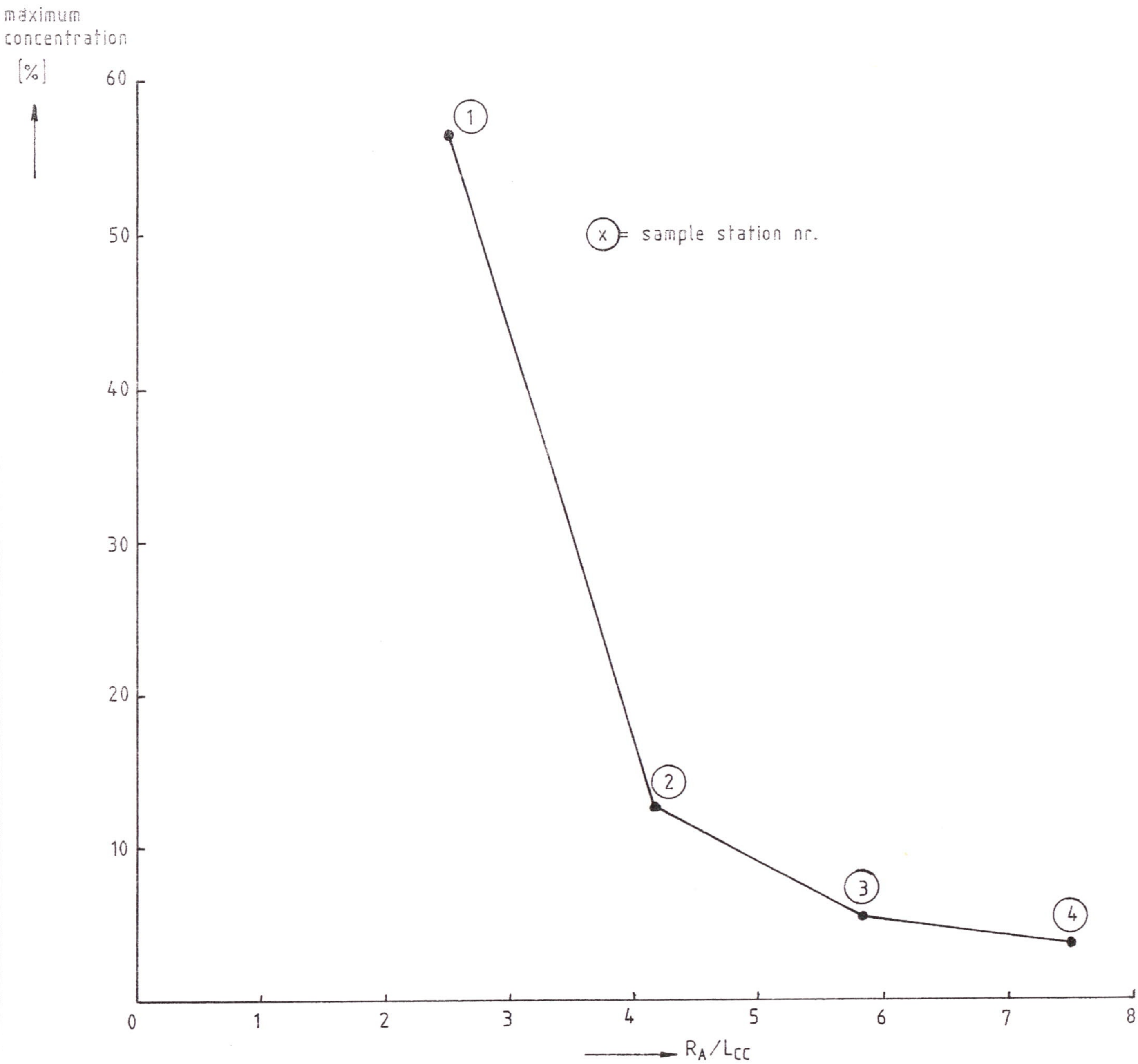

Maximum concentrations for the instantaneous release at line A (see figure 6).

MT-TNO
90-346
Fig.11a

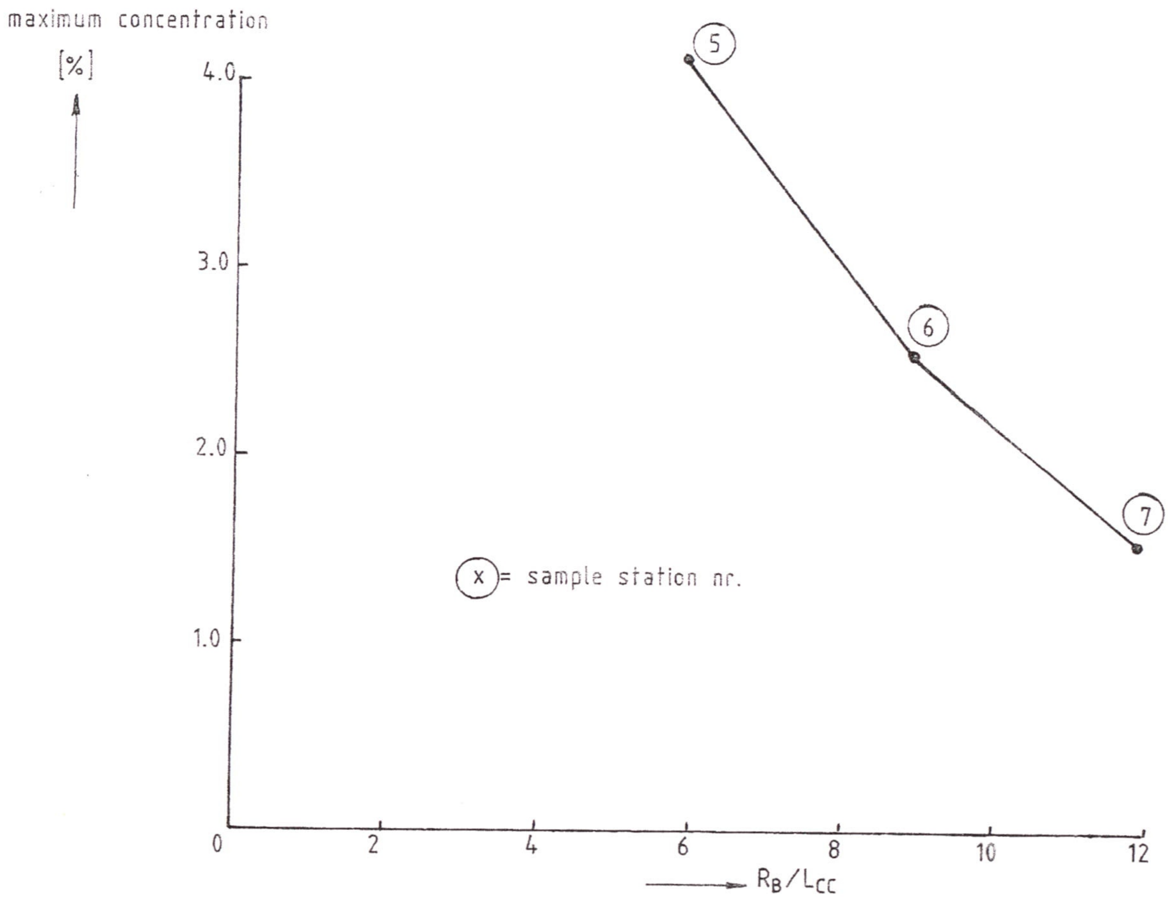

Maximum concentrations for the instantaneous release at line B, (see figure 6).

MT-TNO
90-346
Fig.11b

12a)

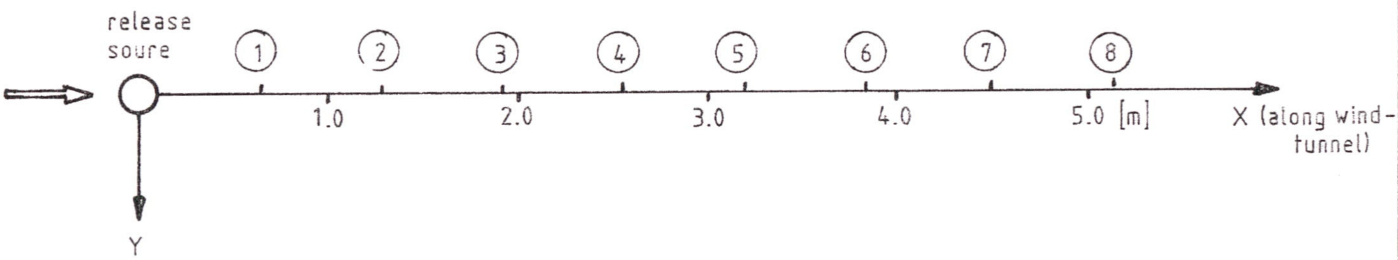

12b)

a) Situation of the probes for the continuous test.
b) Sampling stations for the continuous test.

MT-TNO
90-346
Fig.12a & 12b

Continuous Release

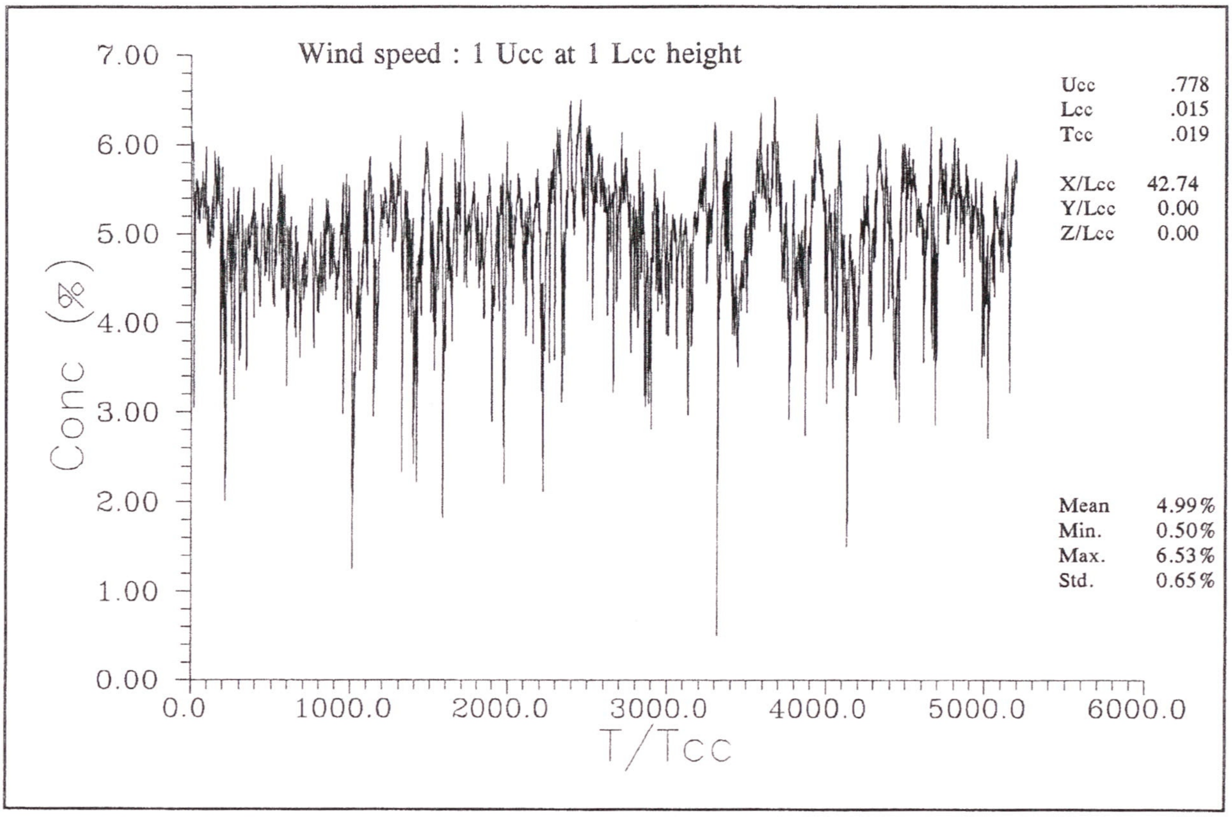

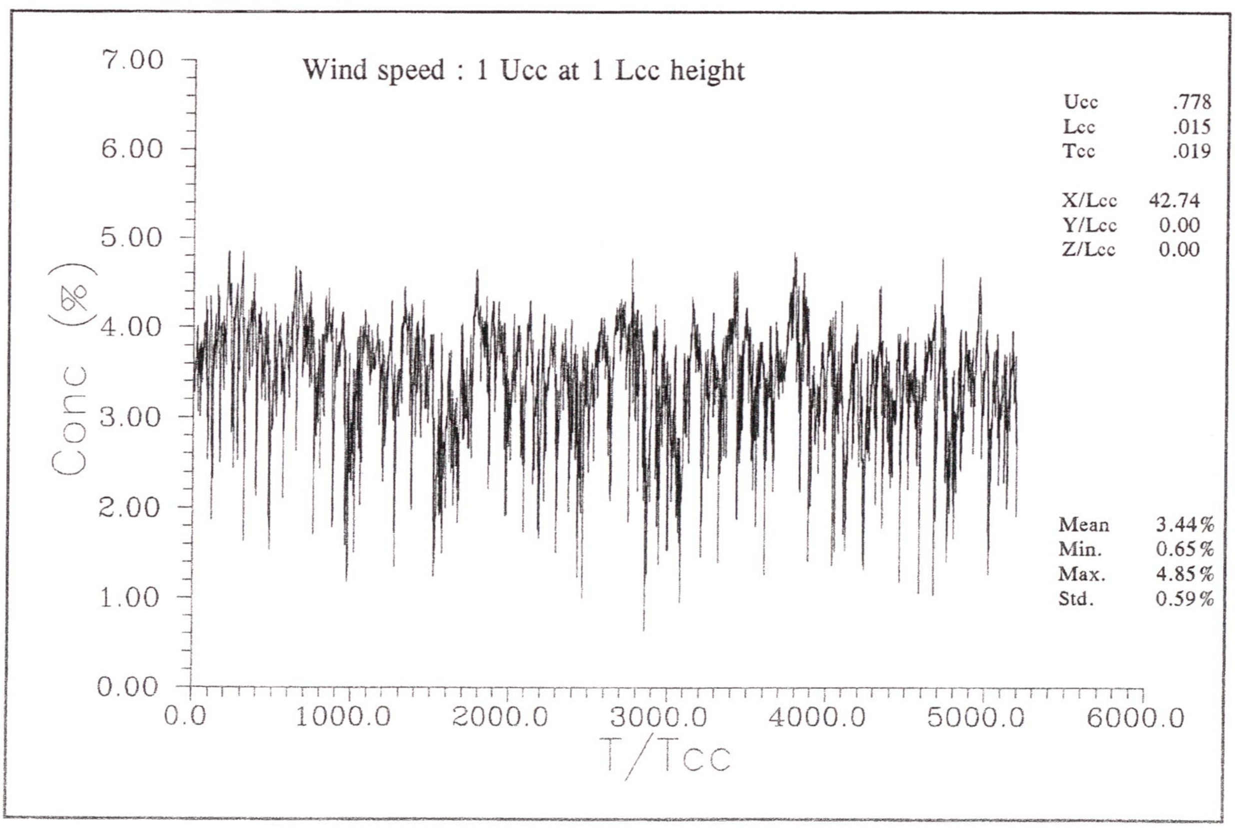

Figure 13 Results of the Continuous release .

Continuous Release

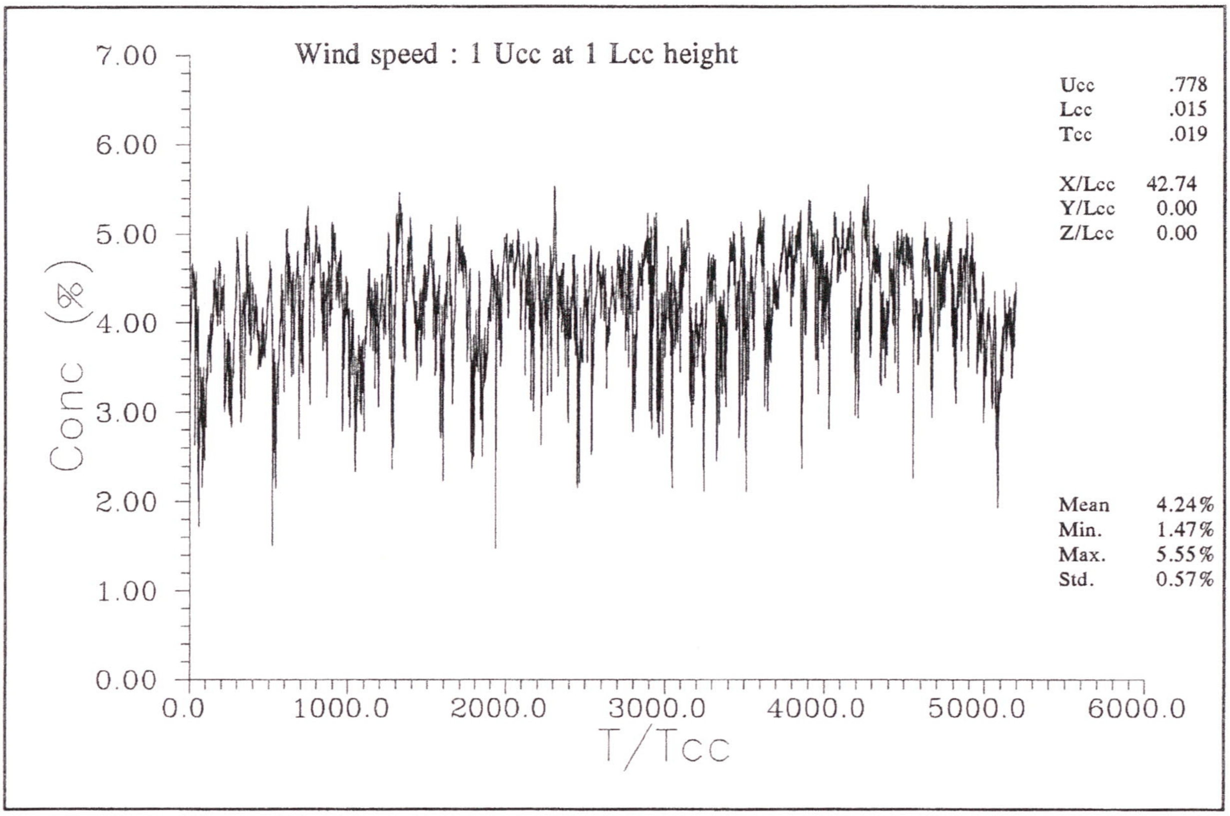

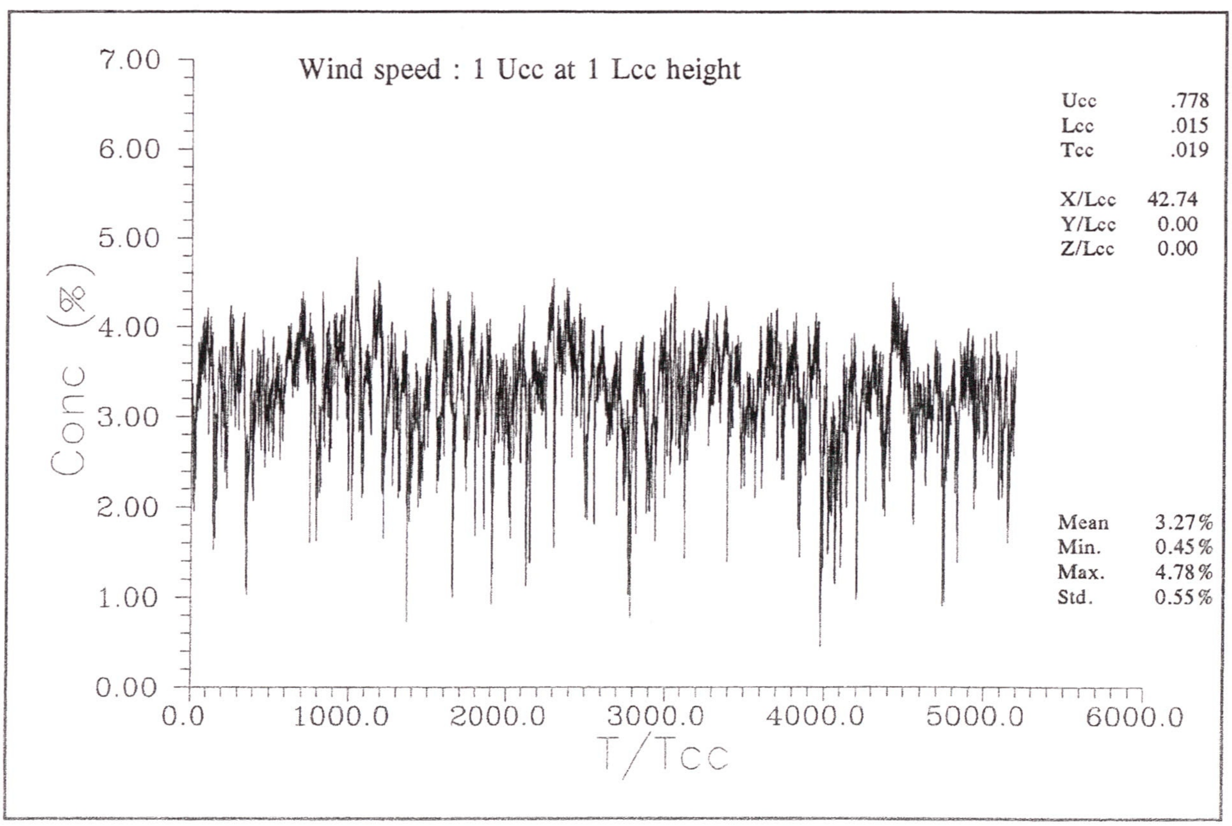

Figure 14 Results of the Continuous release .

Continuous Release

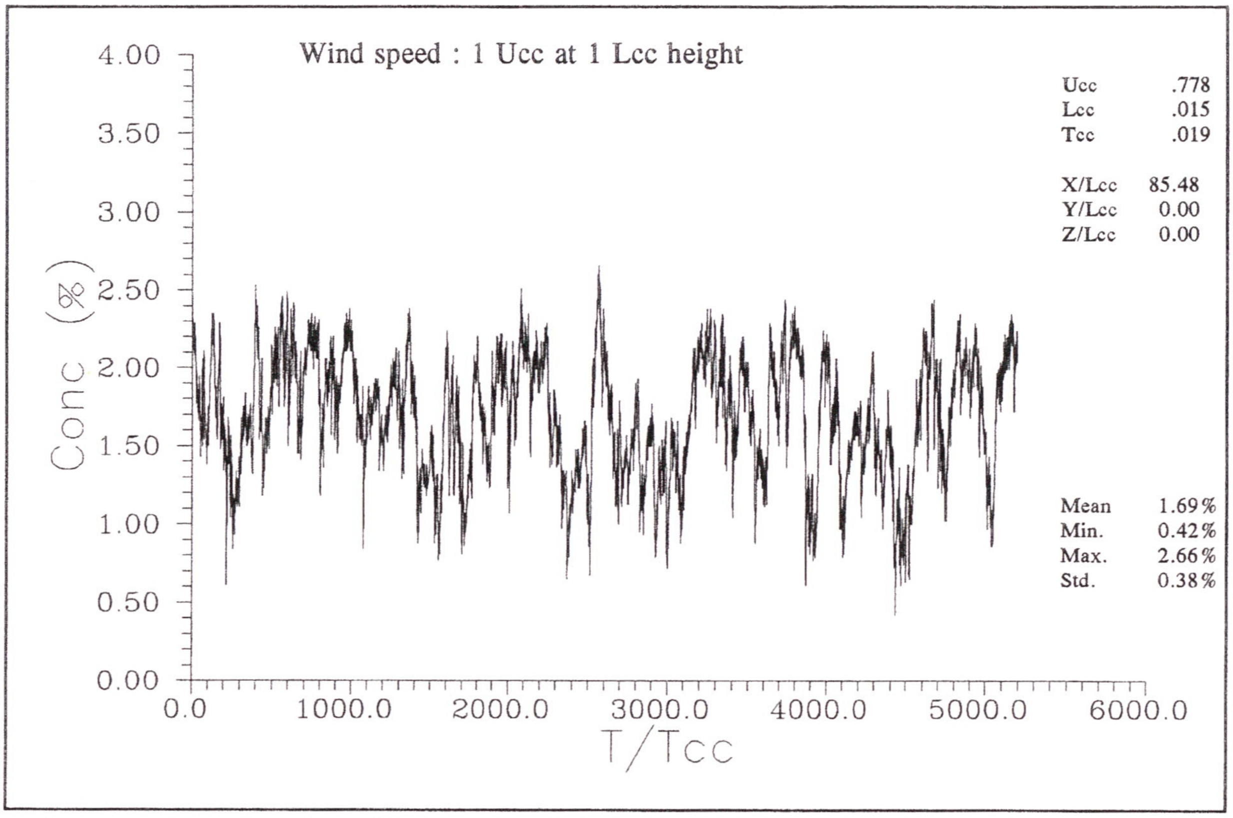

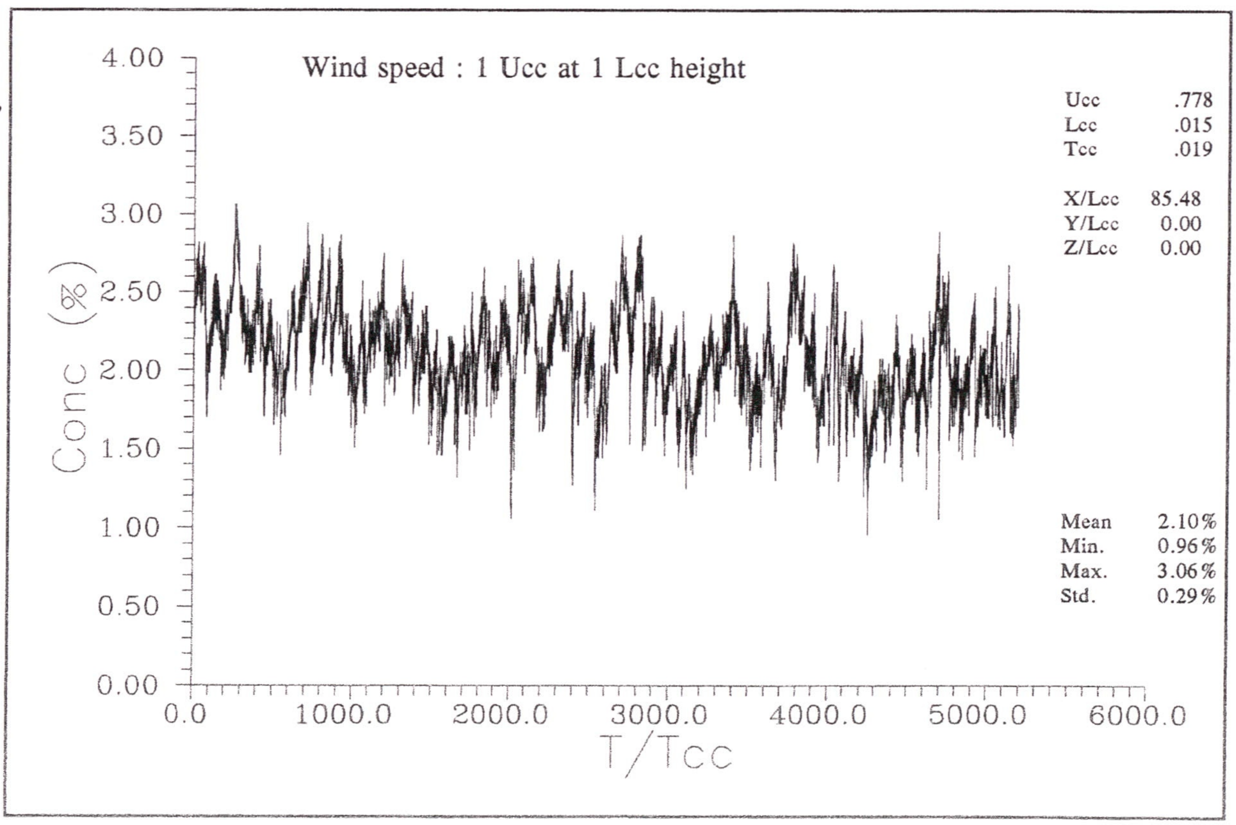

Figure 15 Results of the Continuous release .

Continuous Release

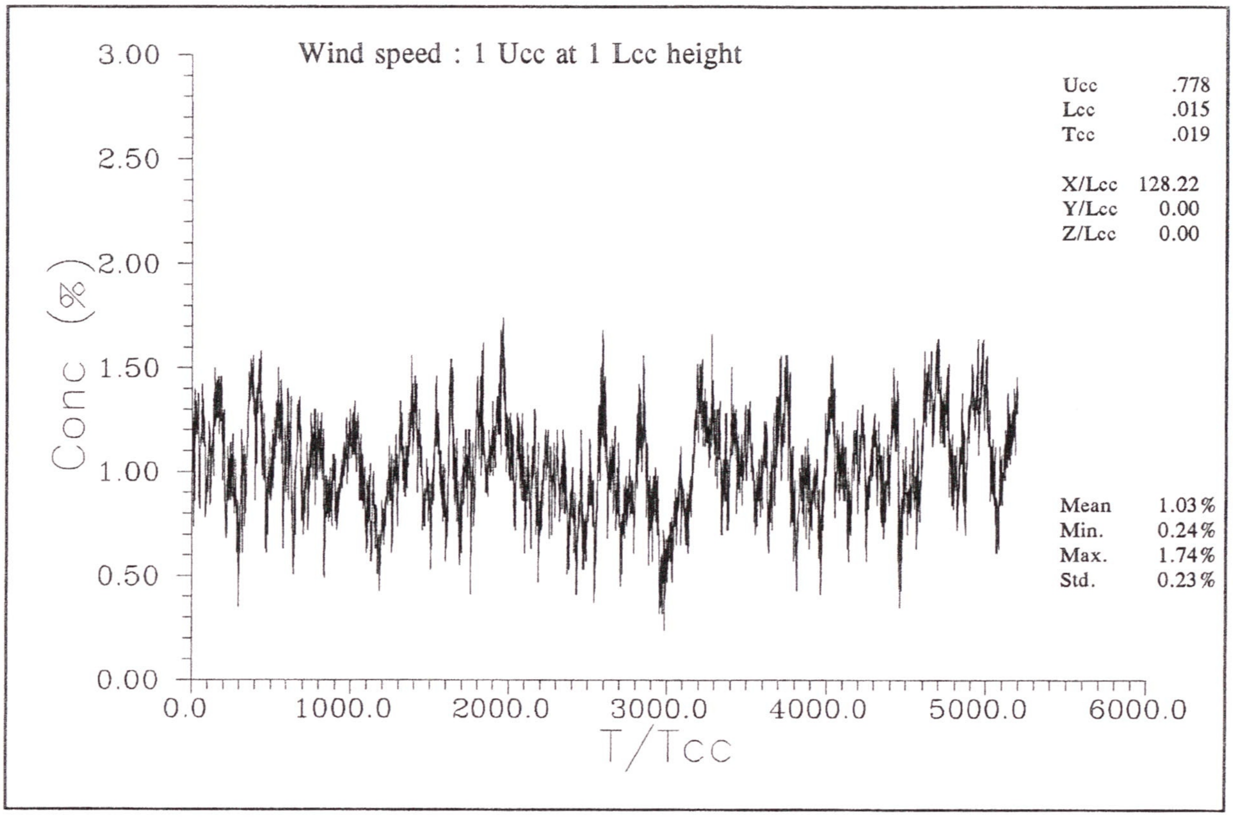

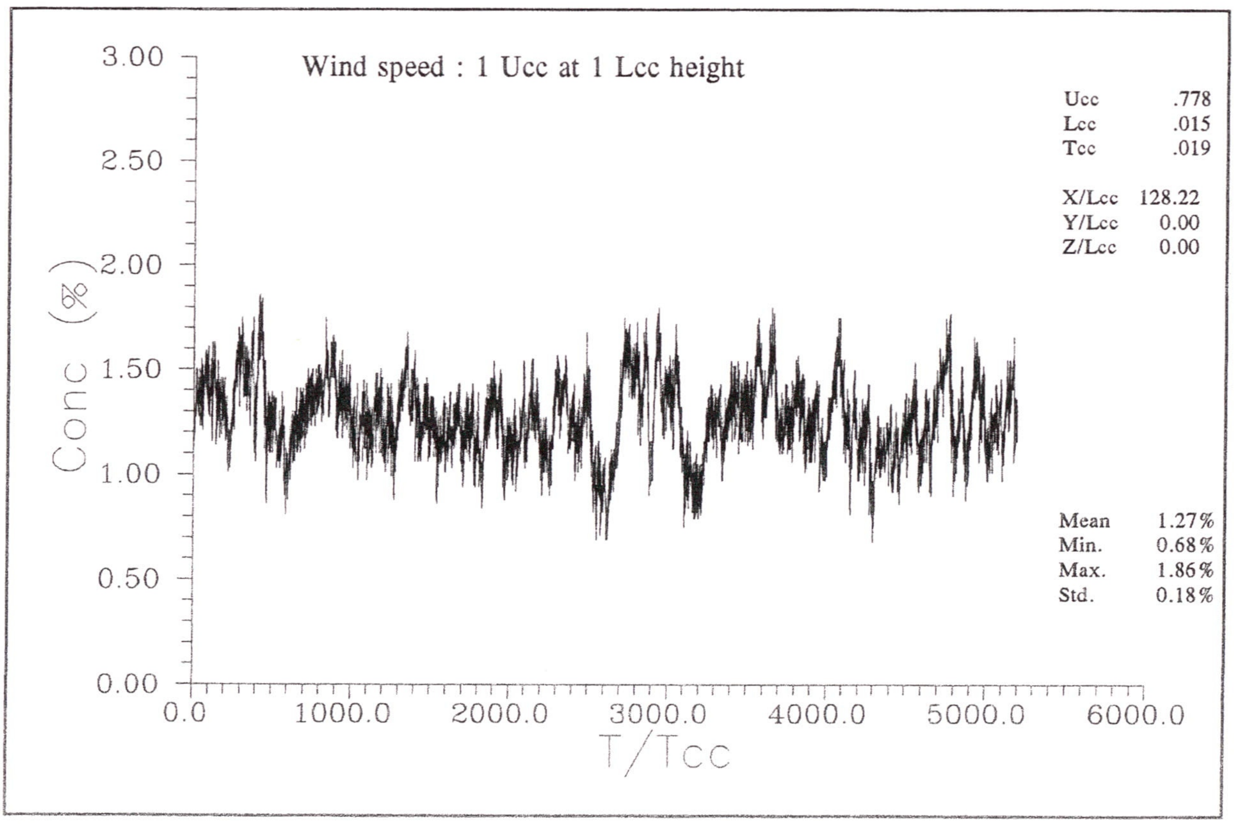

Figure 16 Results of the Continuous release .

Continuous Release

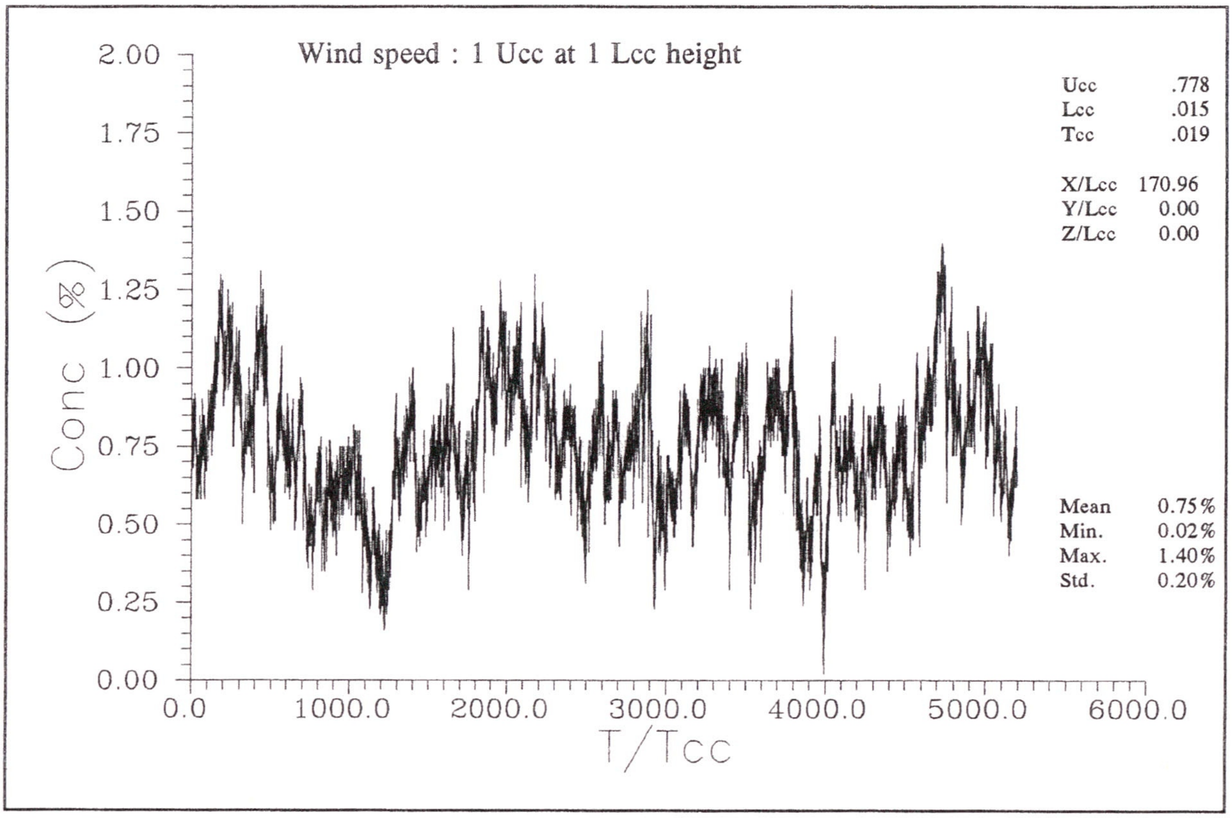

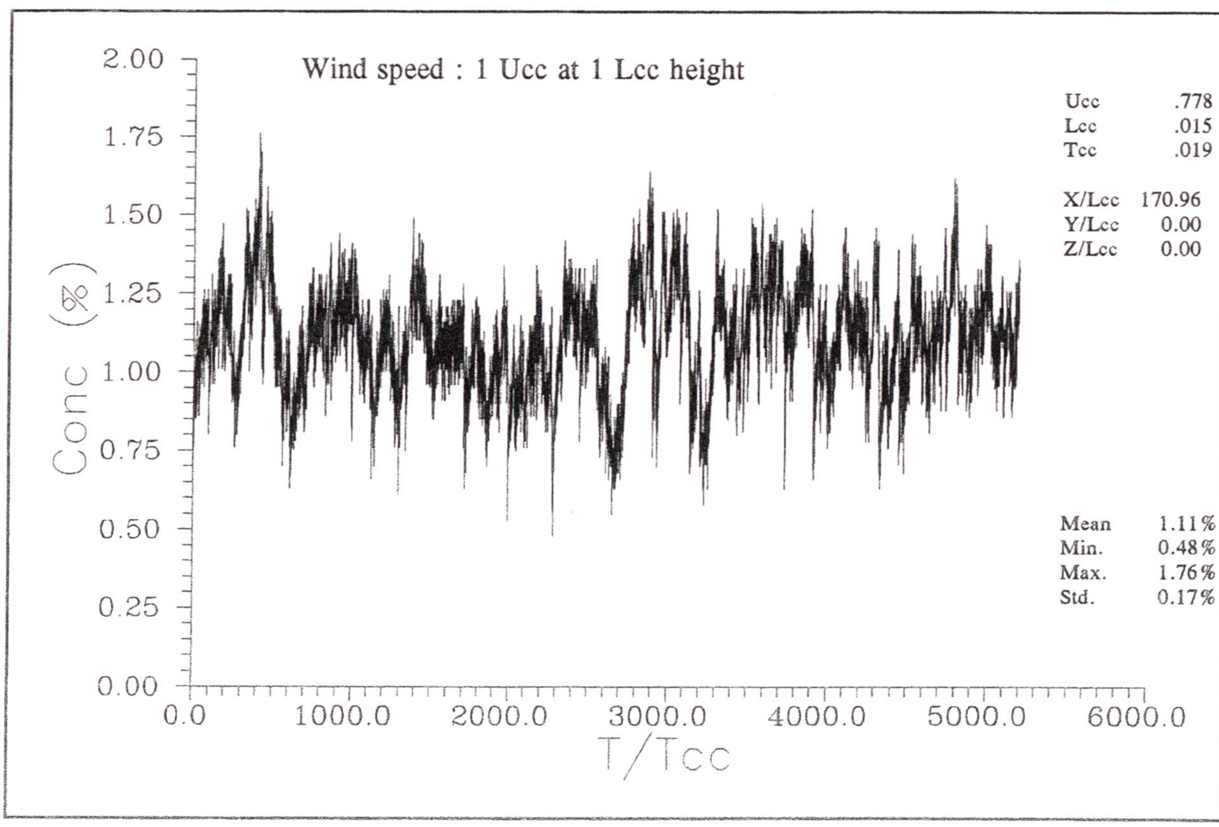

Figure 17 Results of the Continuous release .

Continuous Release

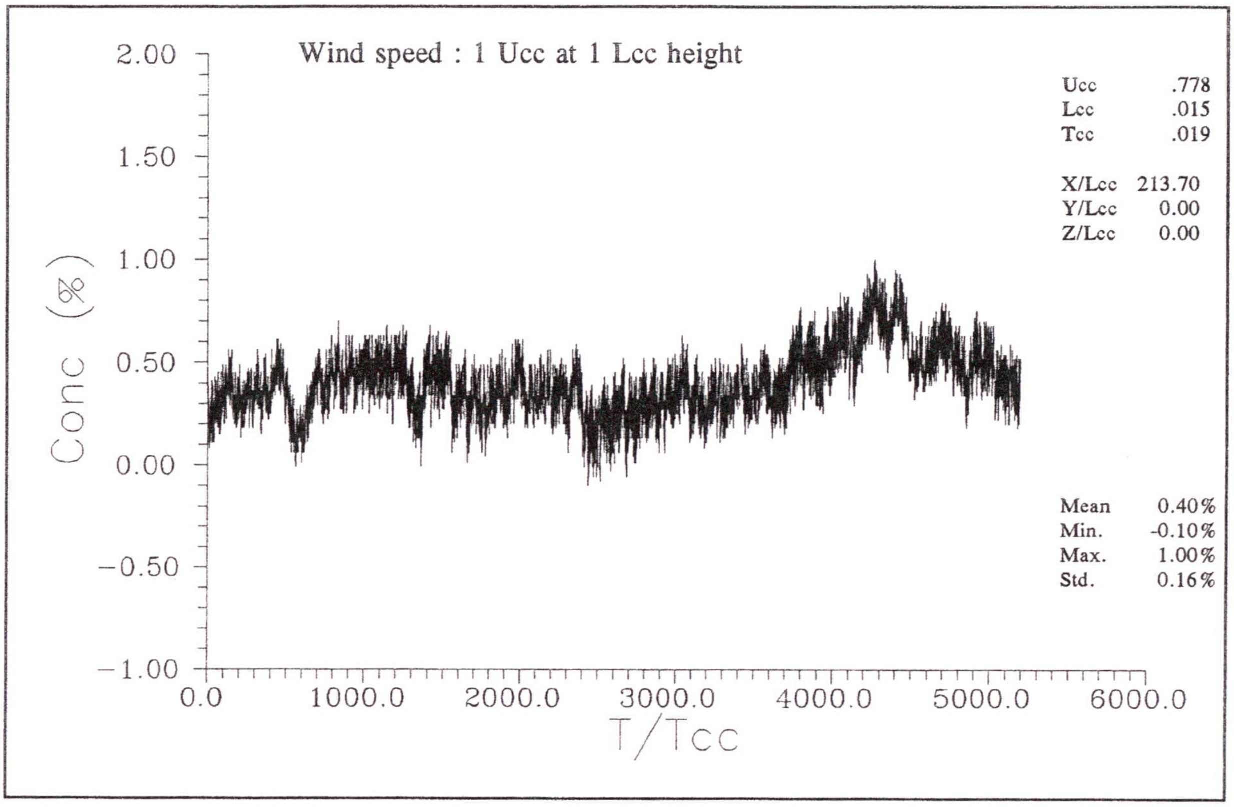

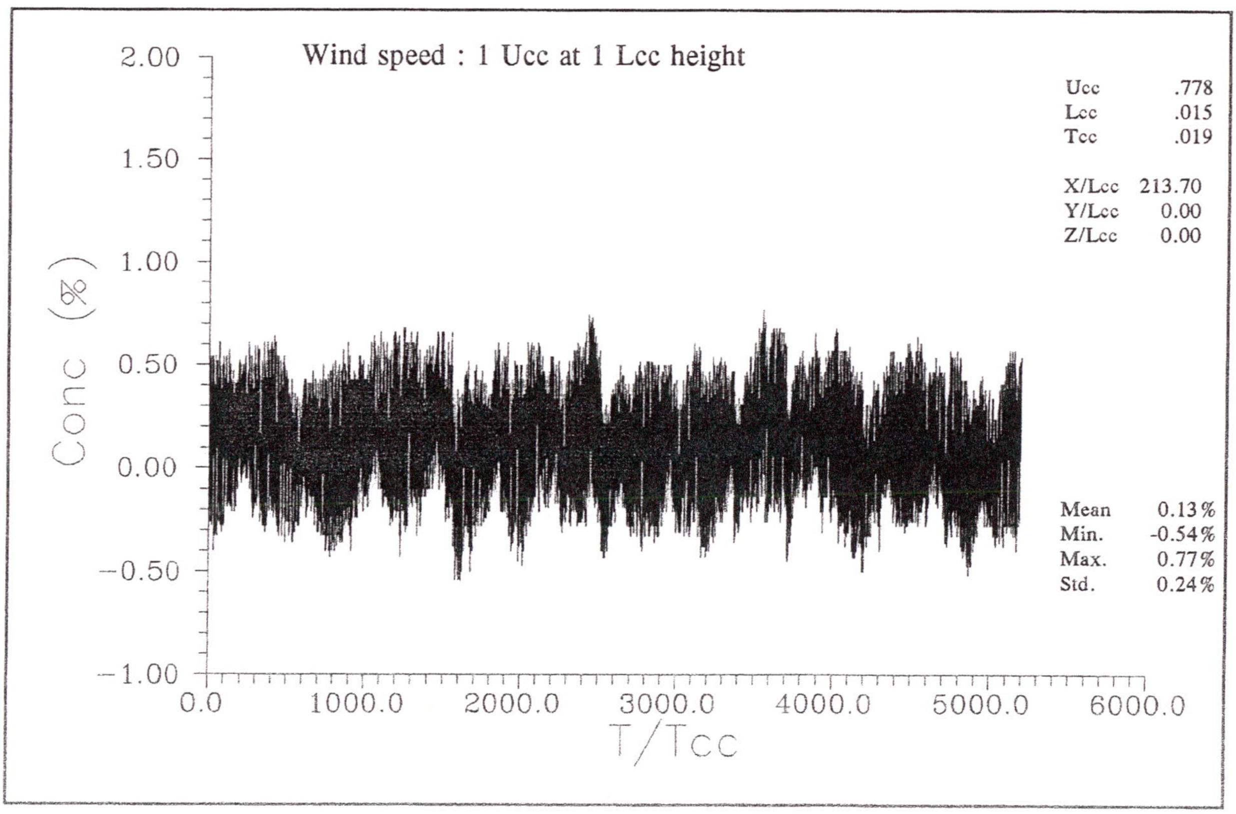

Figure 18 Results of the Continuous release .

Continuous Release

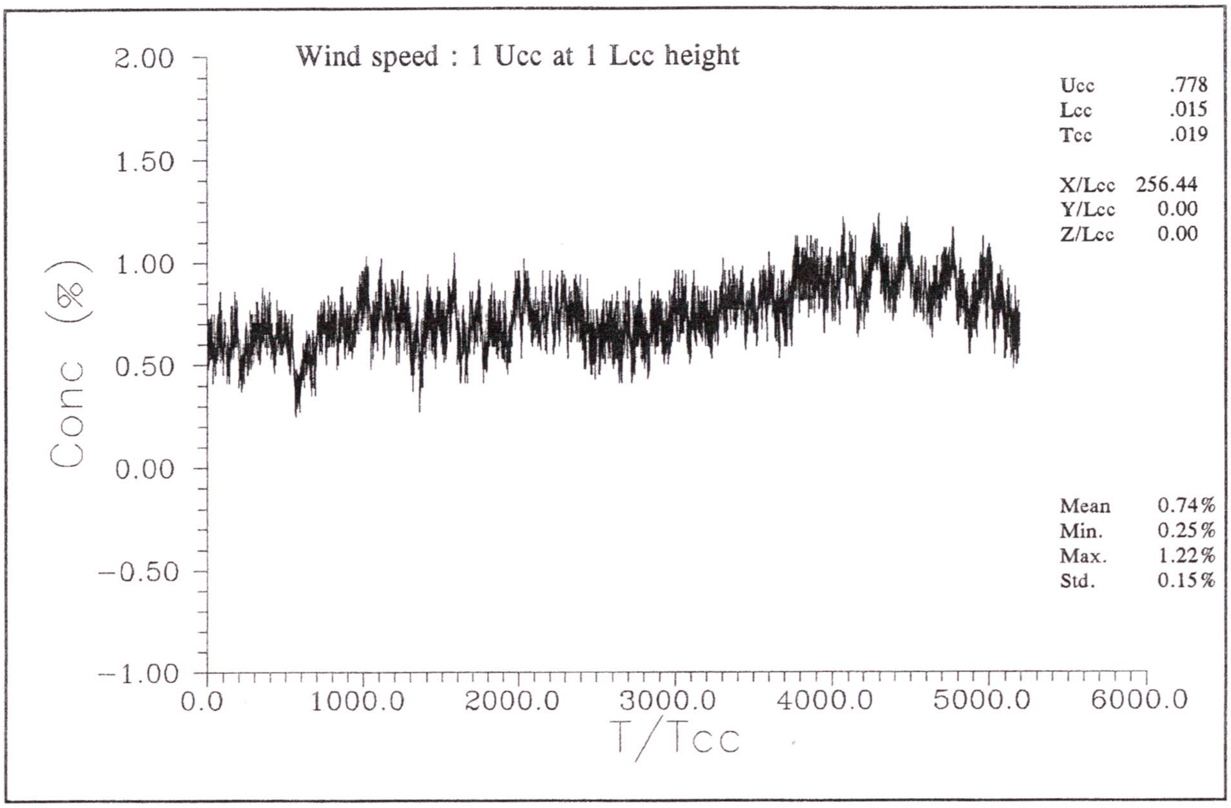

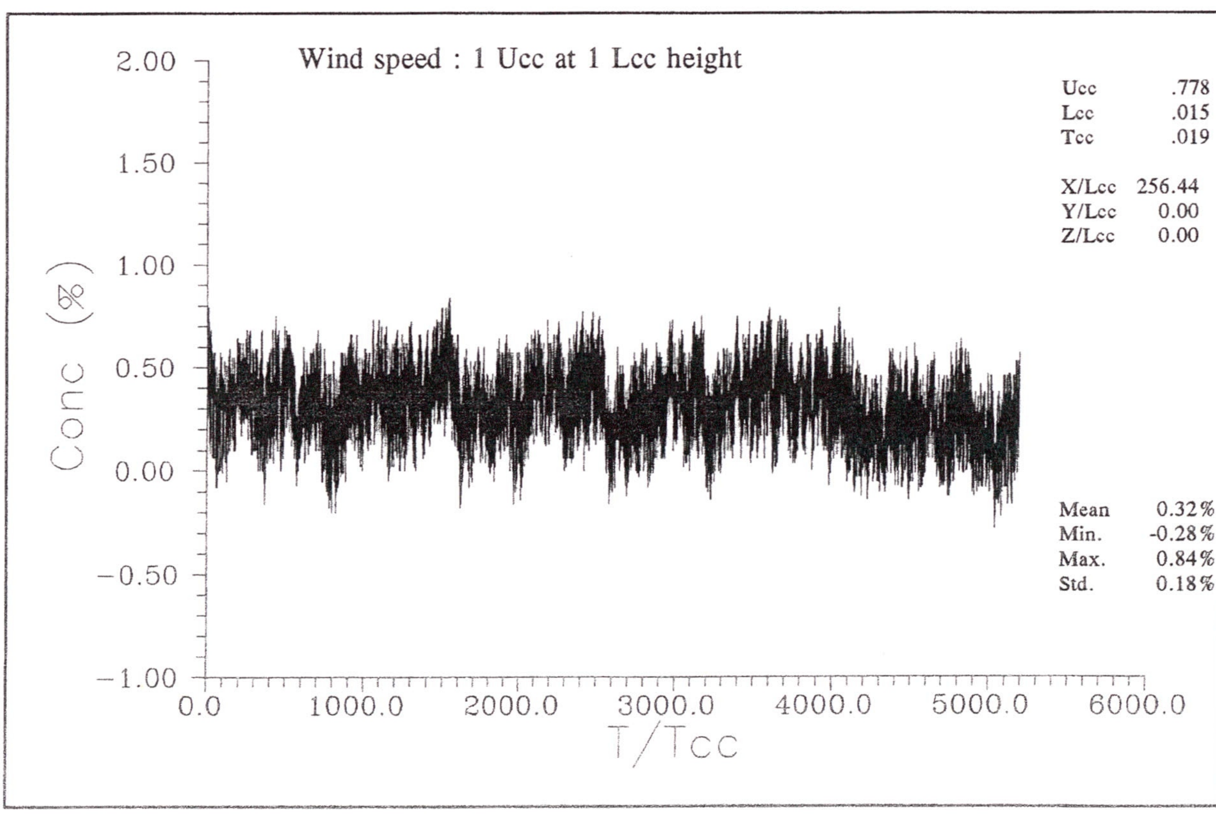

Figure 19 Results of the Continuous release .

Continuous Release

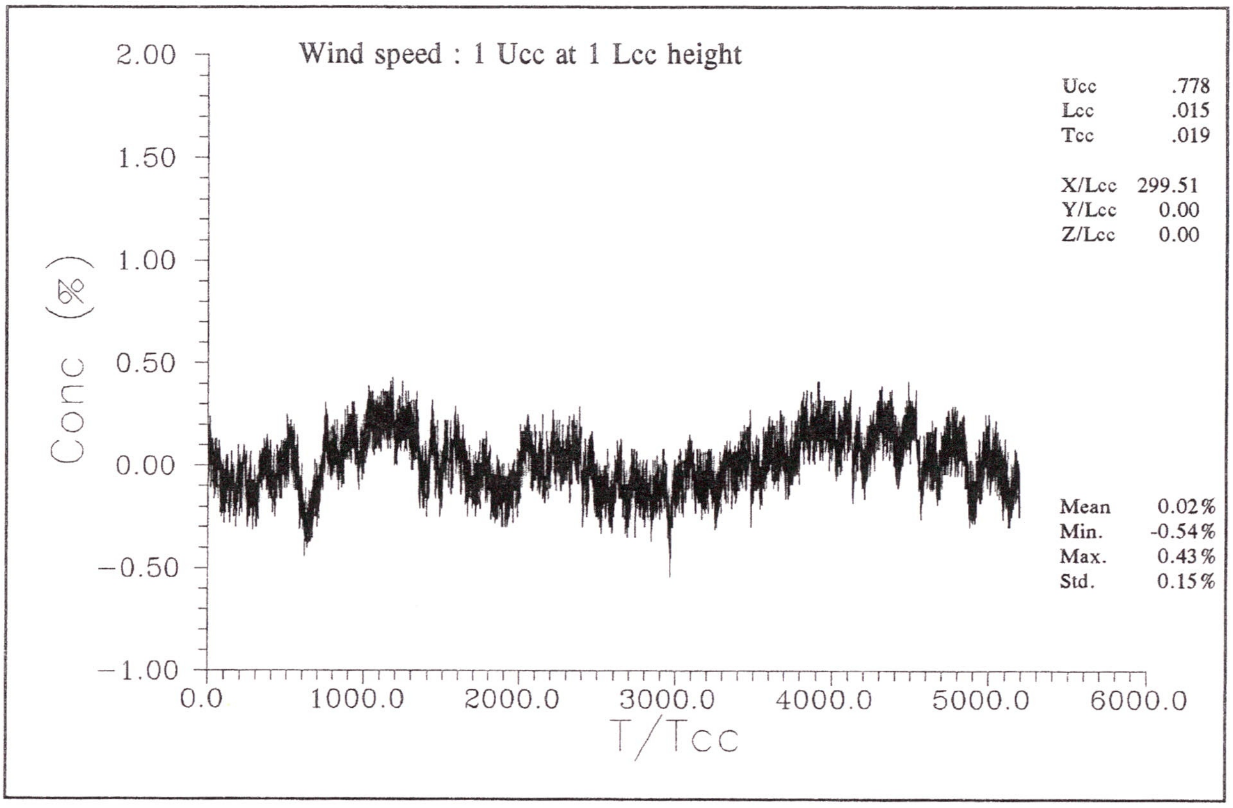

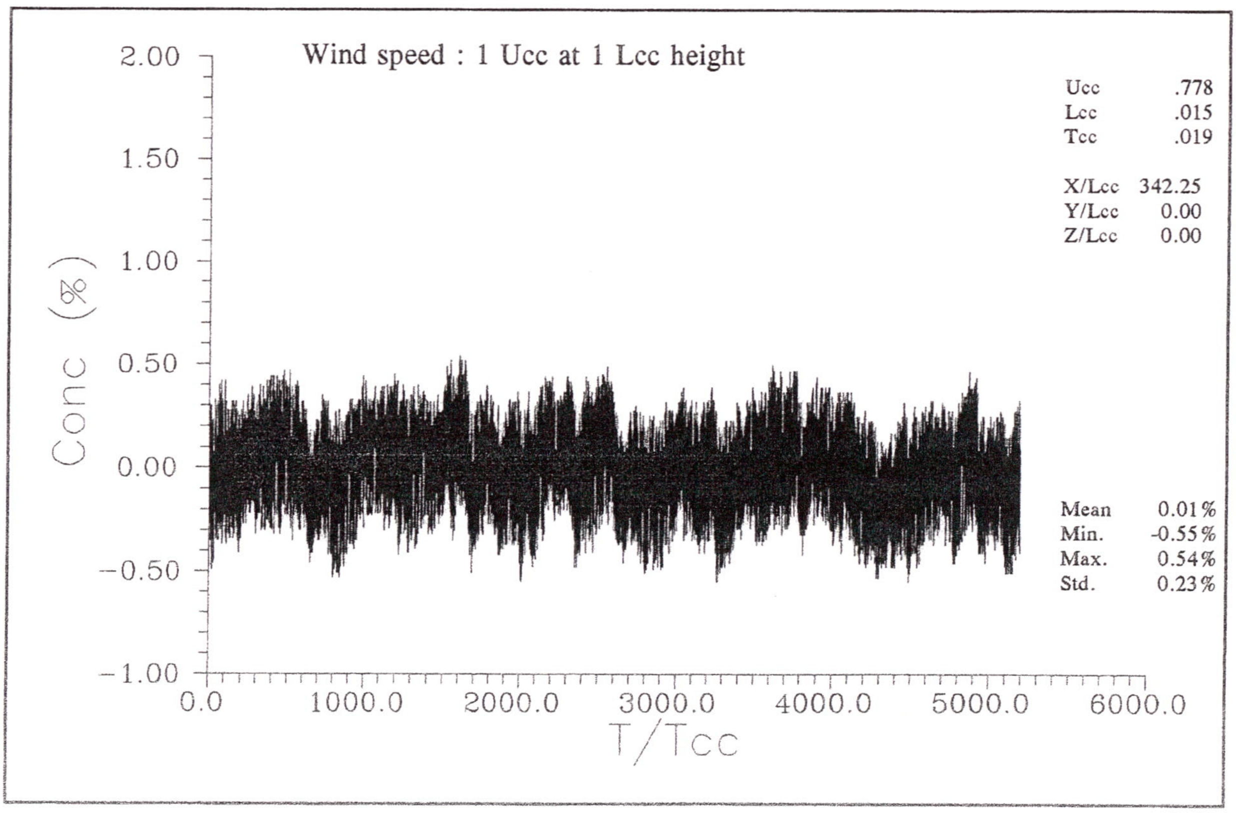

Figure 20 Results of the Continuous release .

Continuous Release

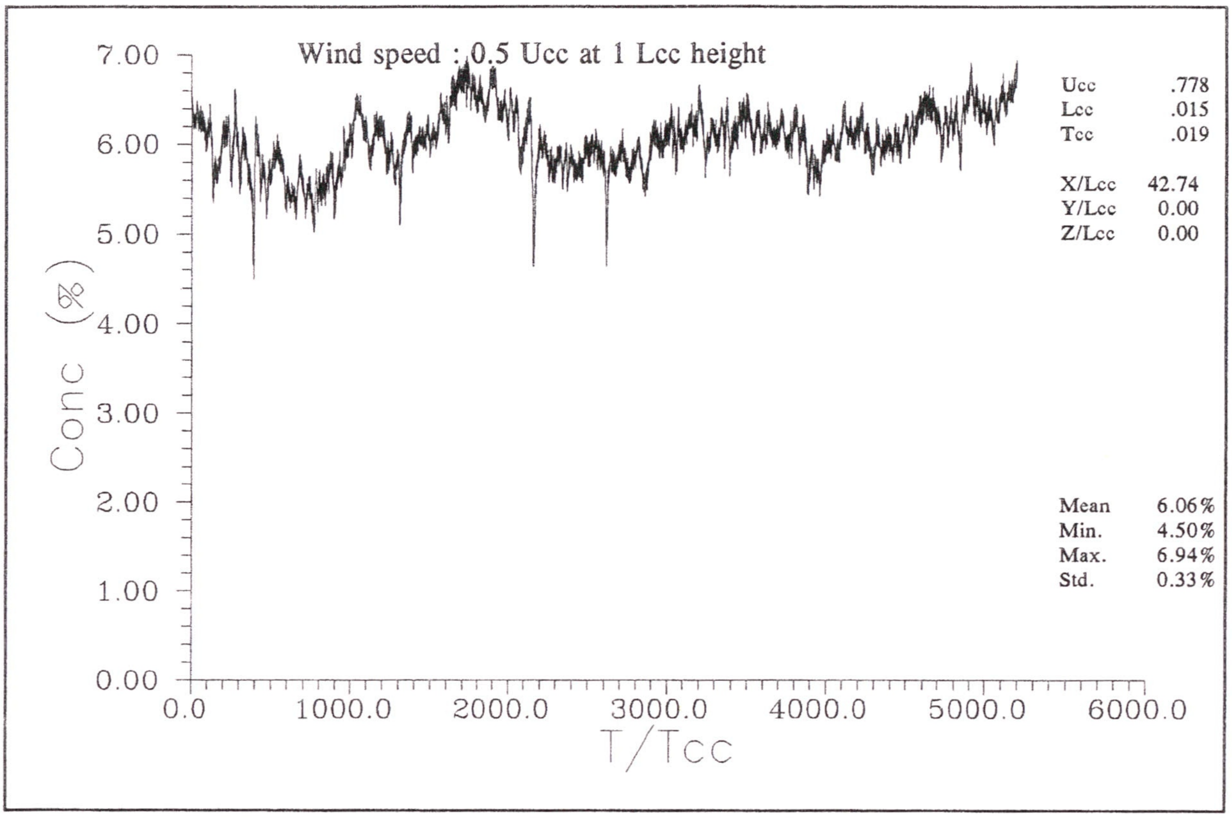

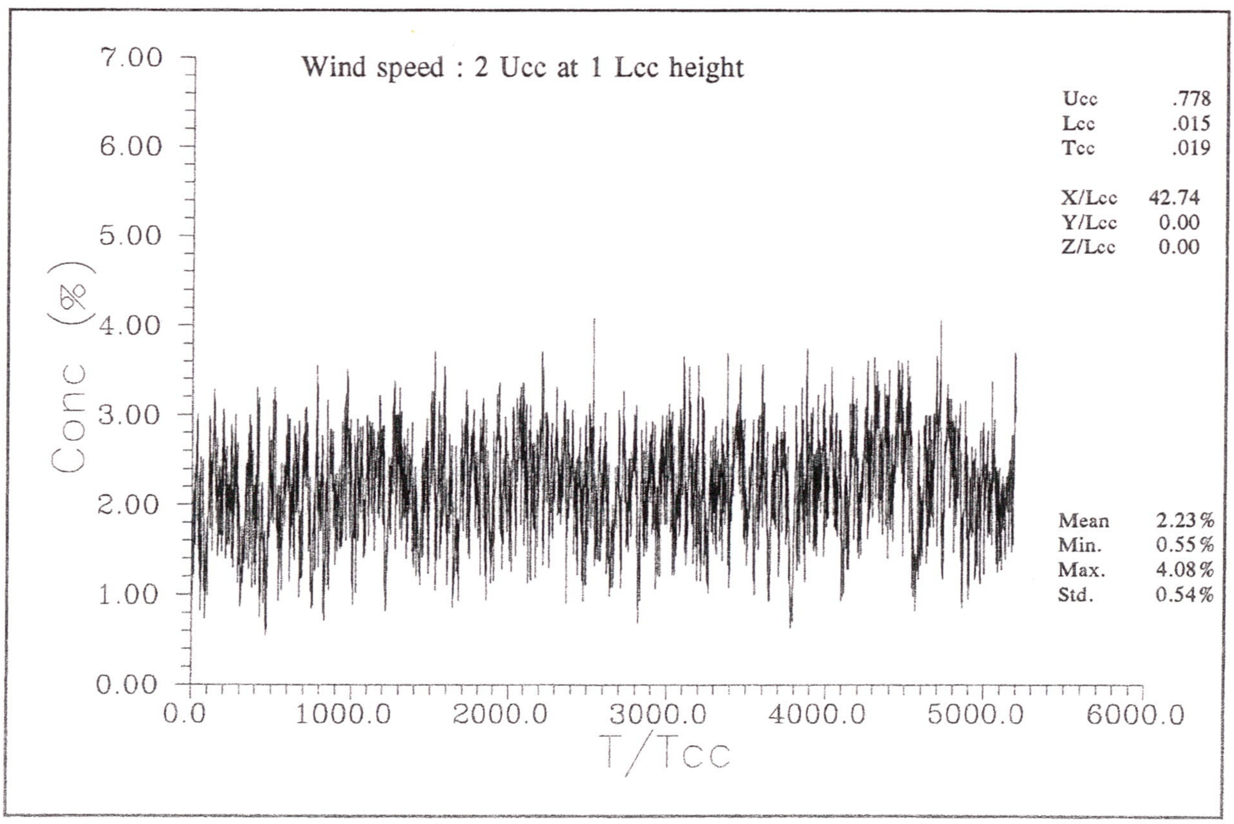

Figure 21 Results of the Continuous release .

Continuous Release

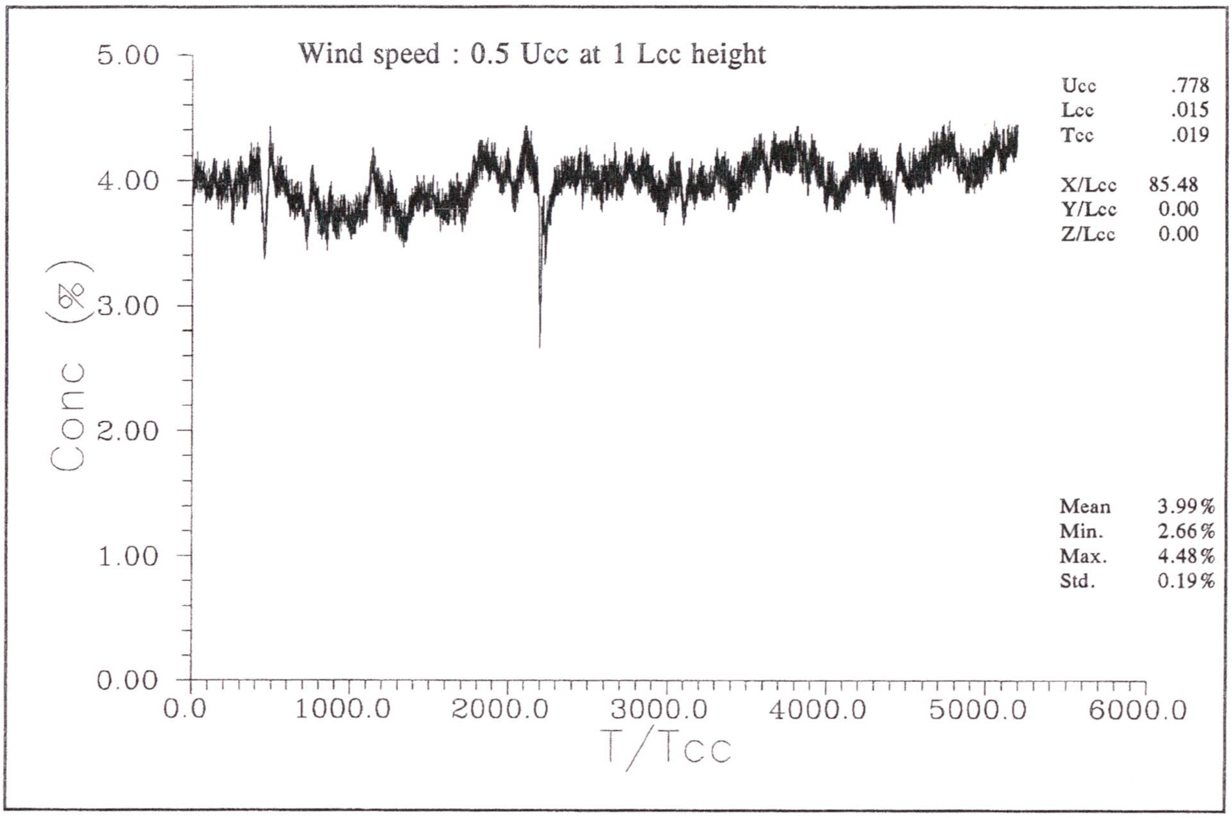

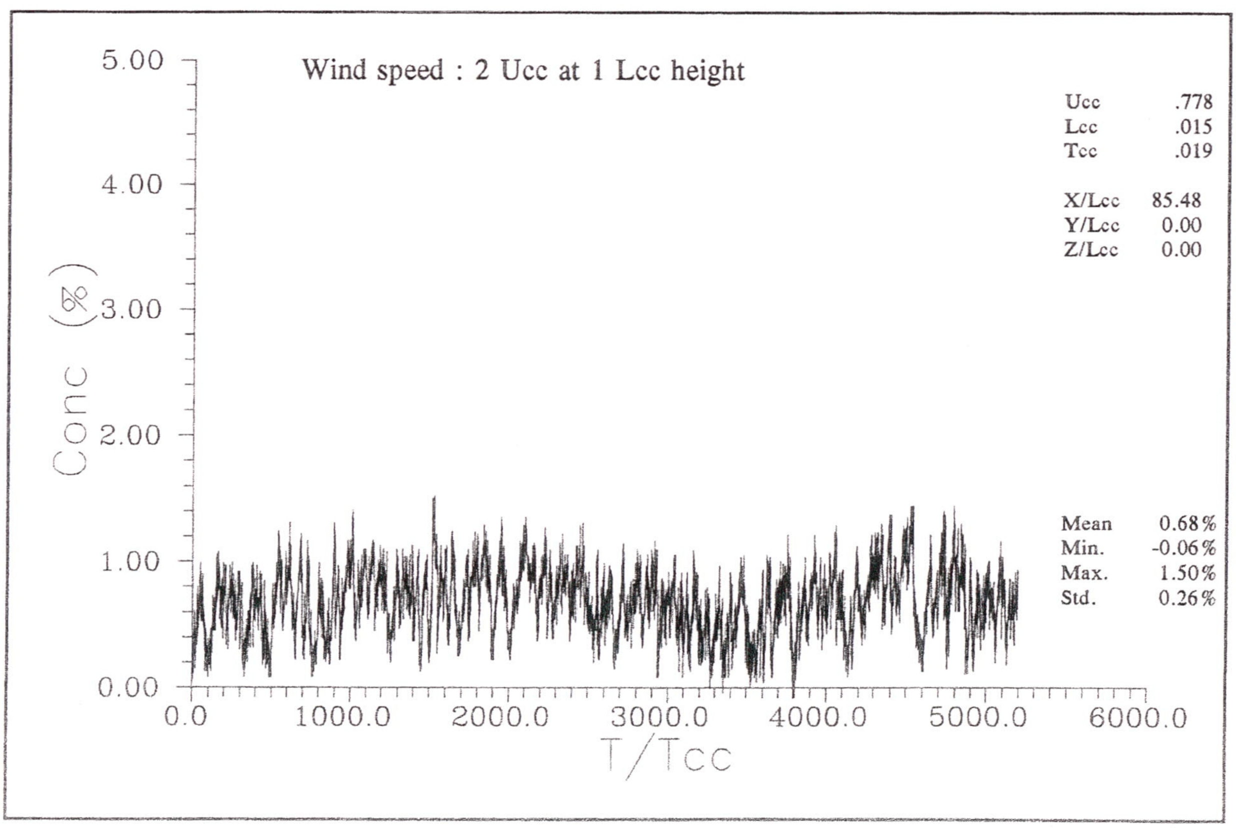

Figure 22 Results of the Continuous release .

Continuous Release

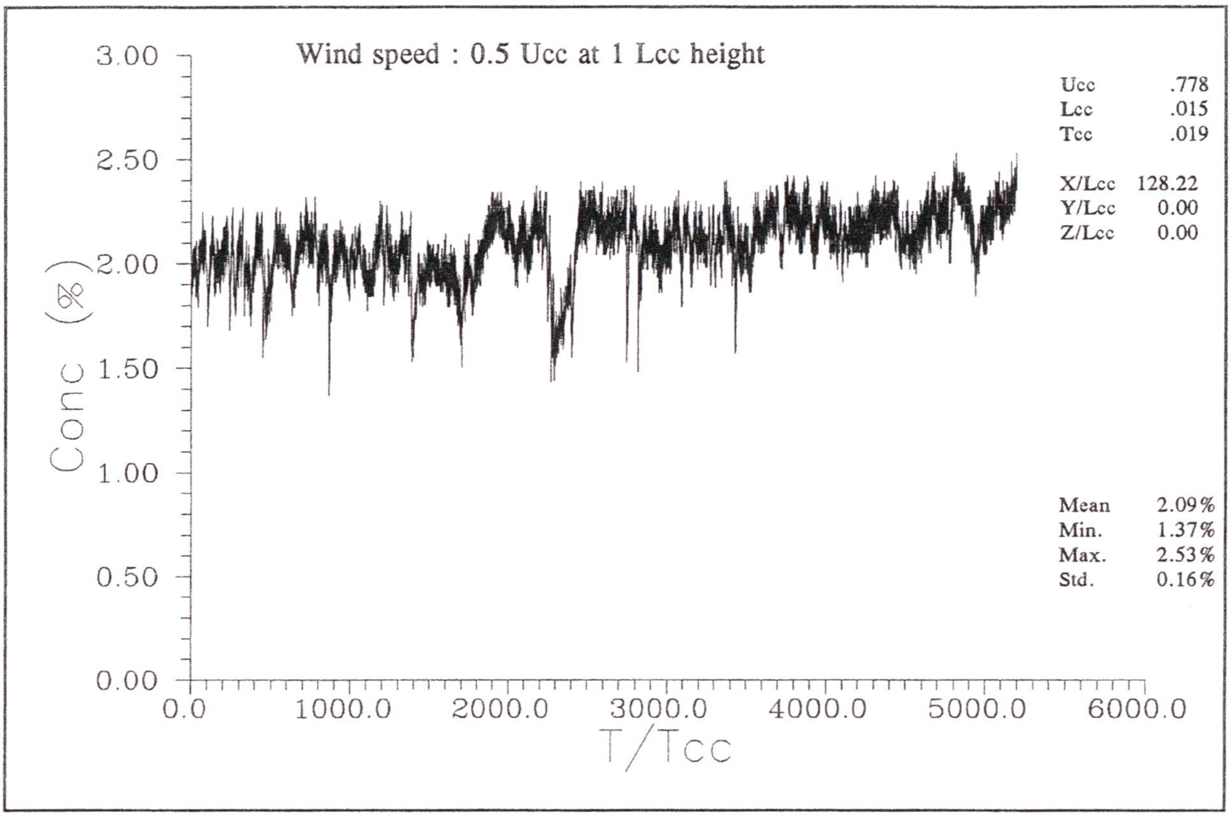

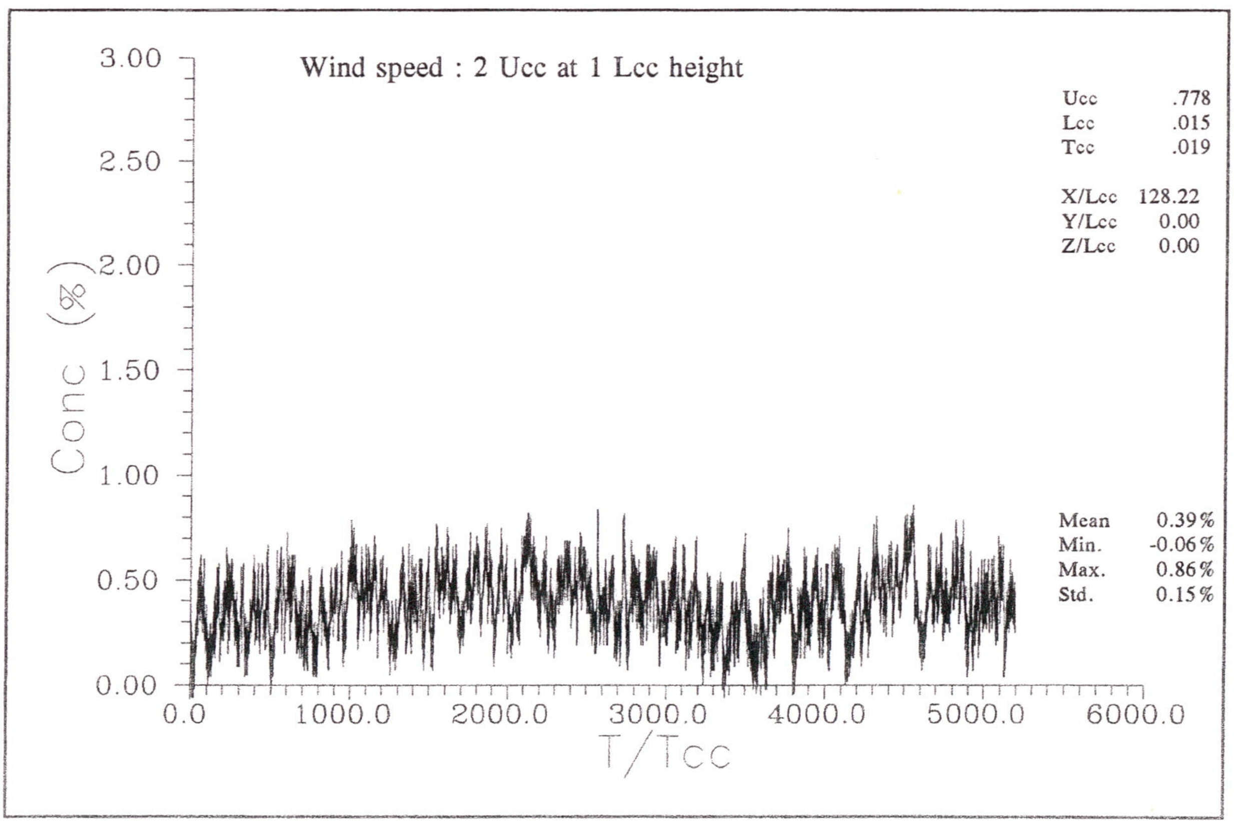

Figure 23 Results of the Continuous release .

Continuous Release

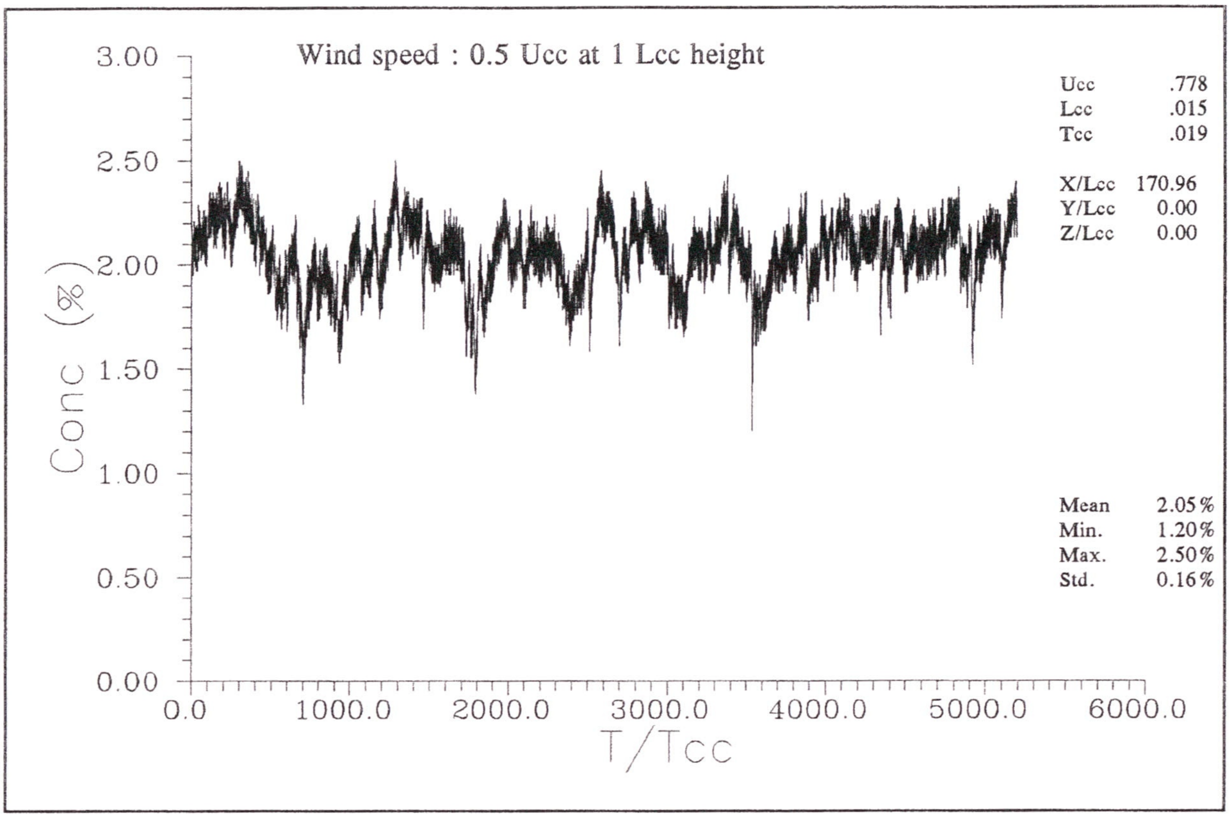

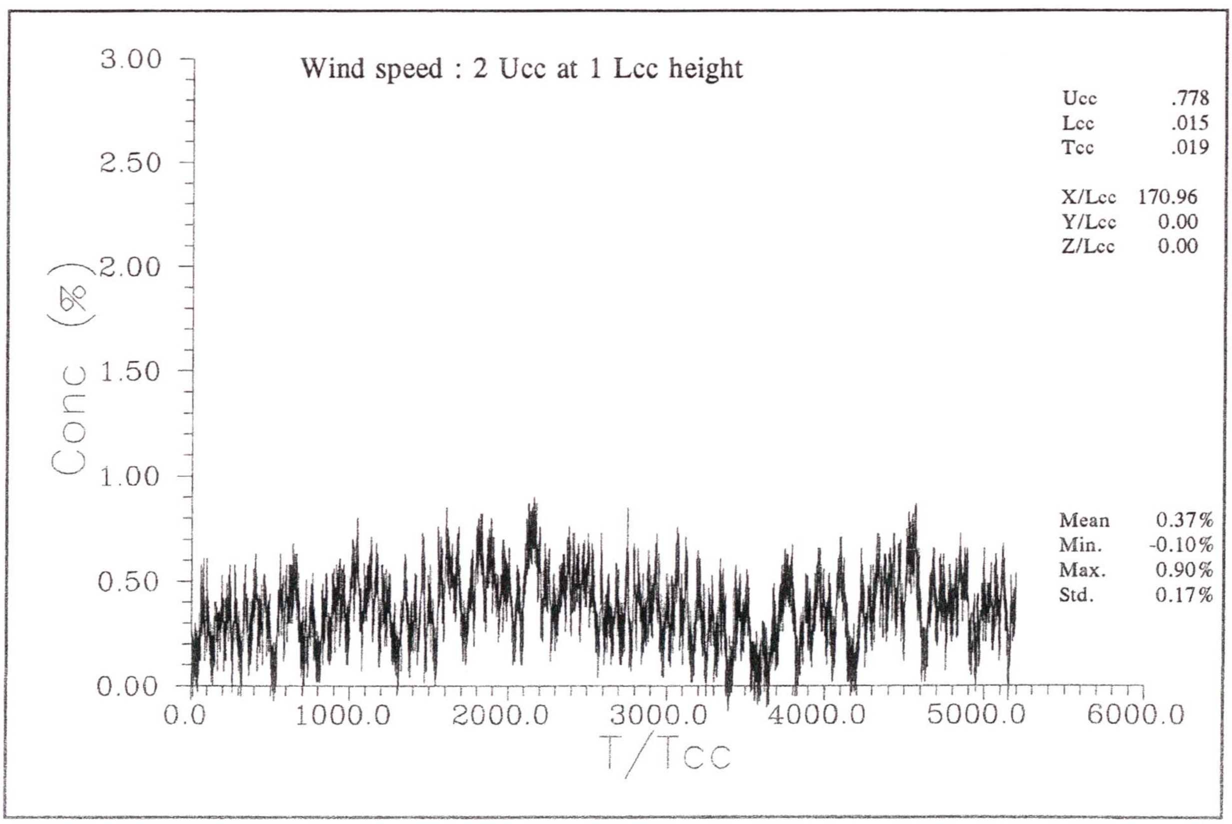

Figure 24 Results of the Continuous release .

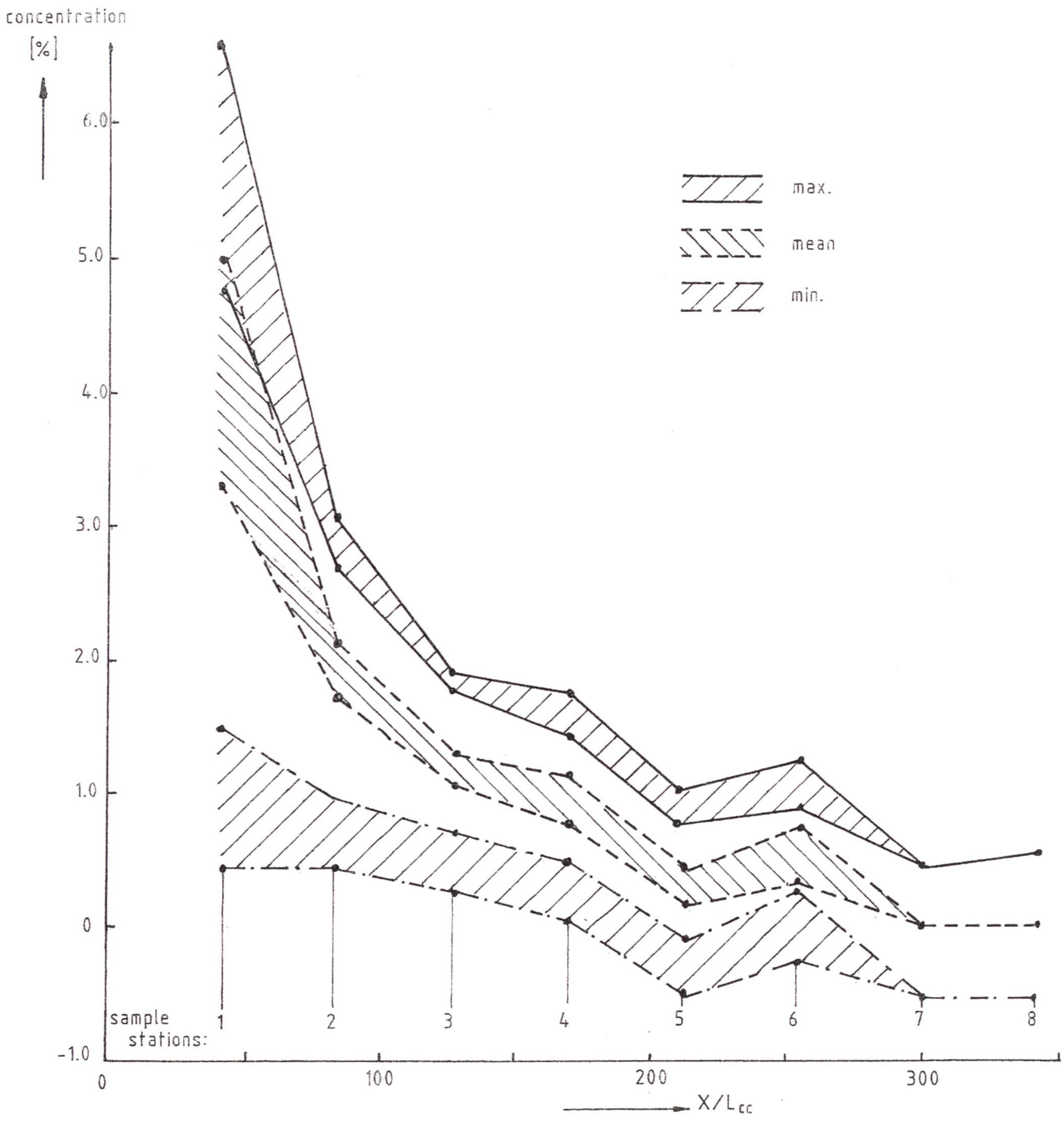

Mean, minimum and maximum concentrations for the continuous release test.	MT-TNO 90-346 Fig.25

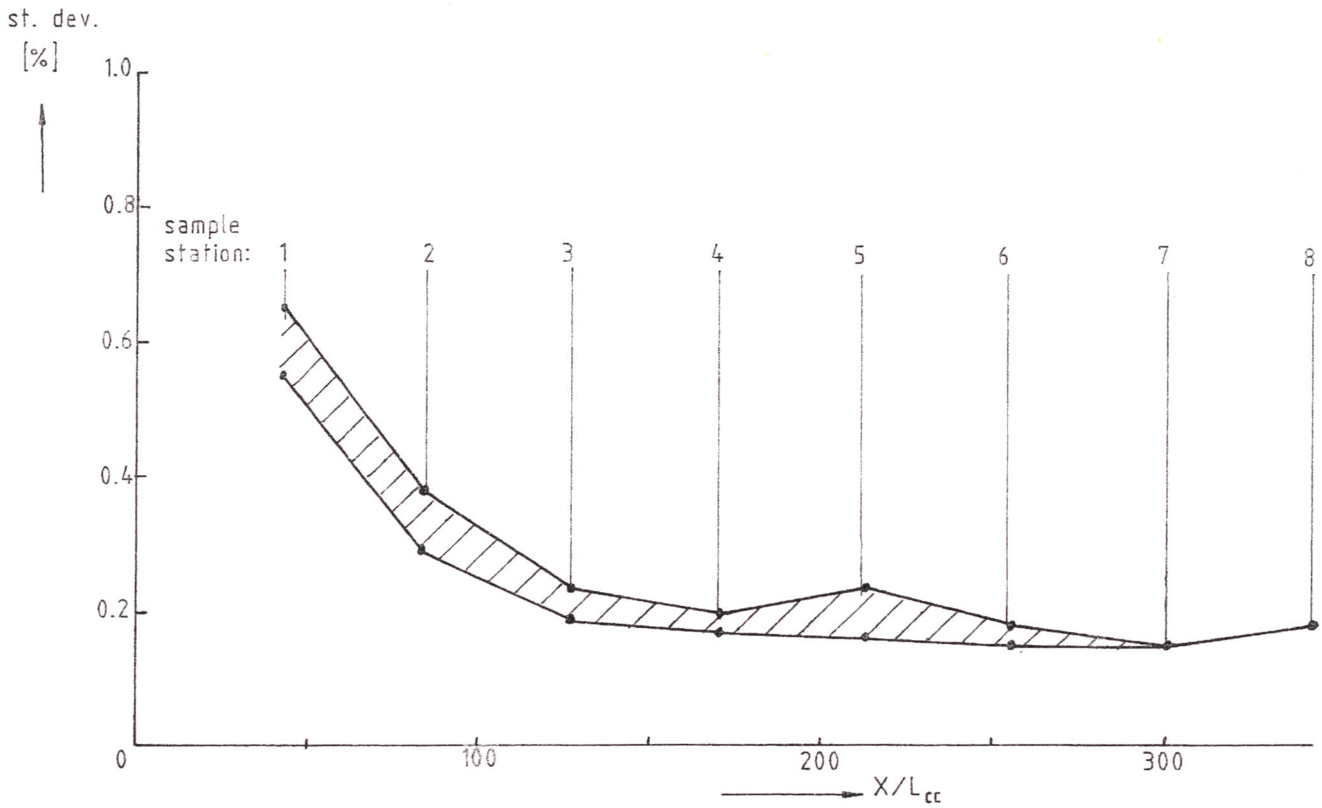

Standard deviation for the continuous release test.	MT-TNO 90-346 Fig.26

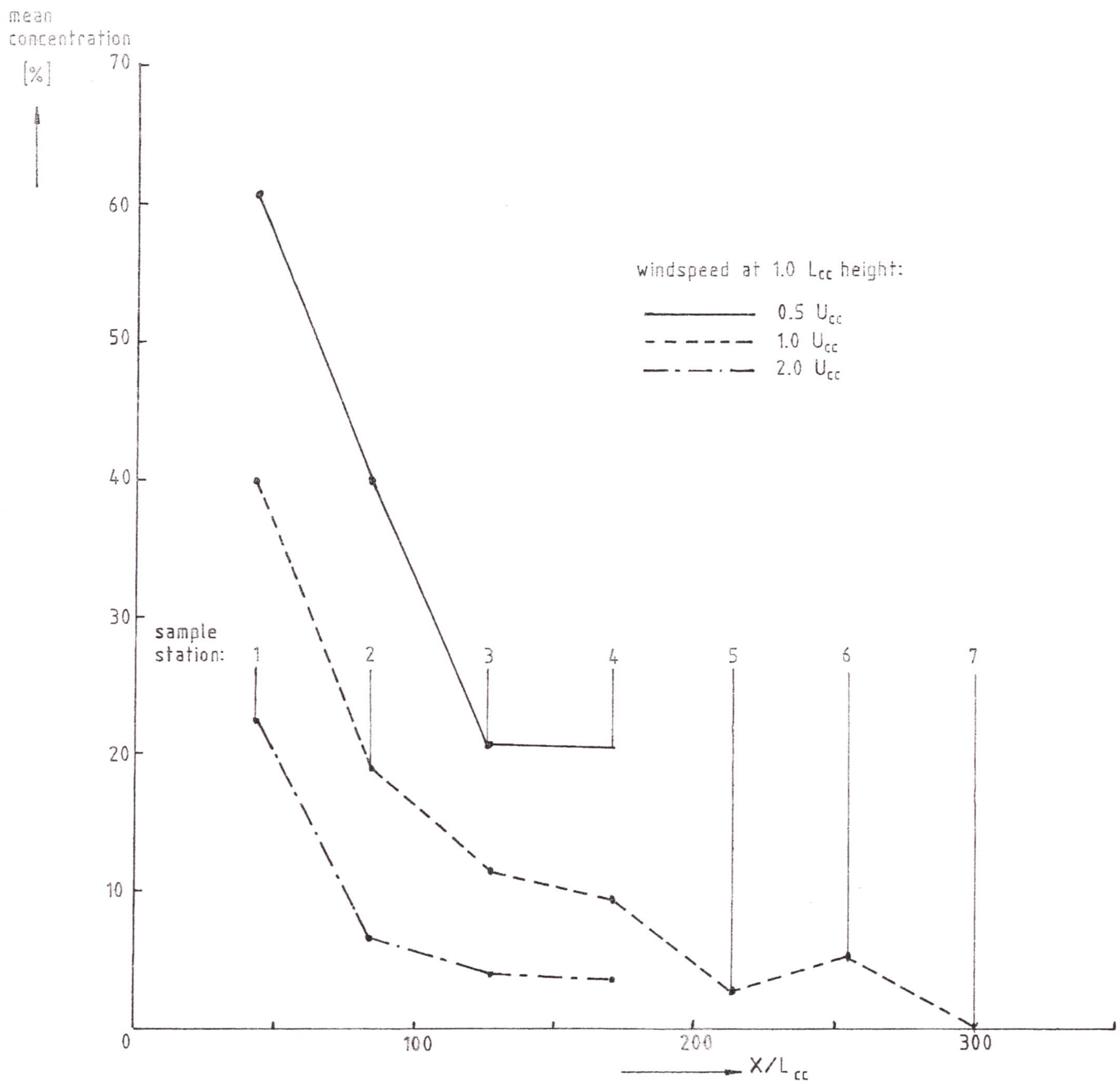

Mean concentration for the intercomparison continuous test and both additional test.

MT-TNO
90-346
Fig.27

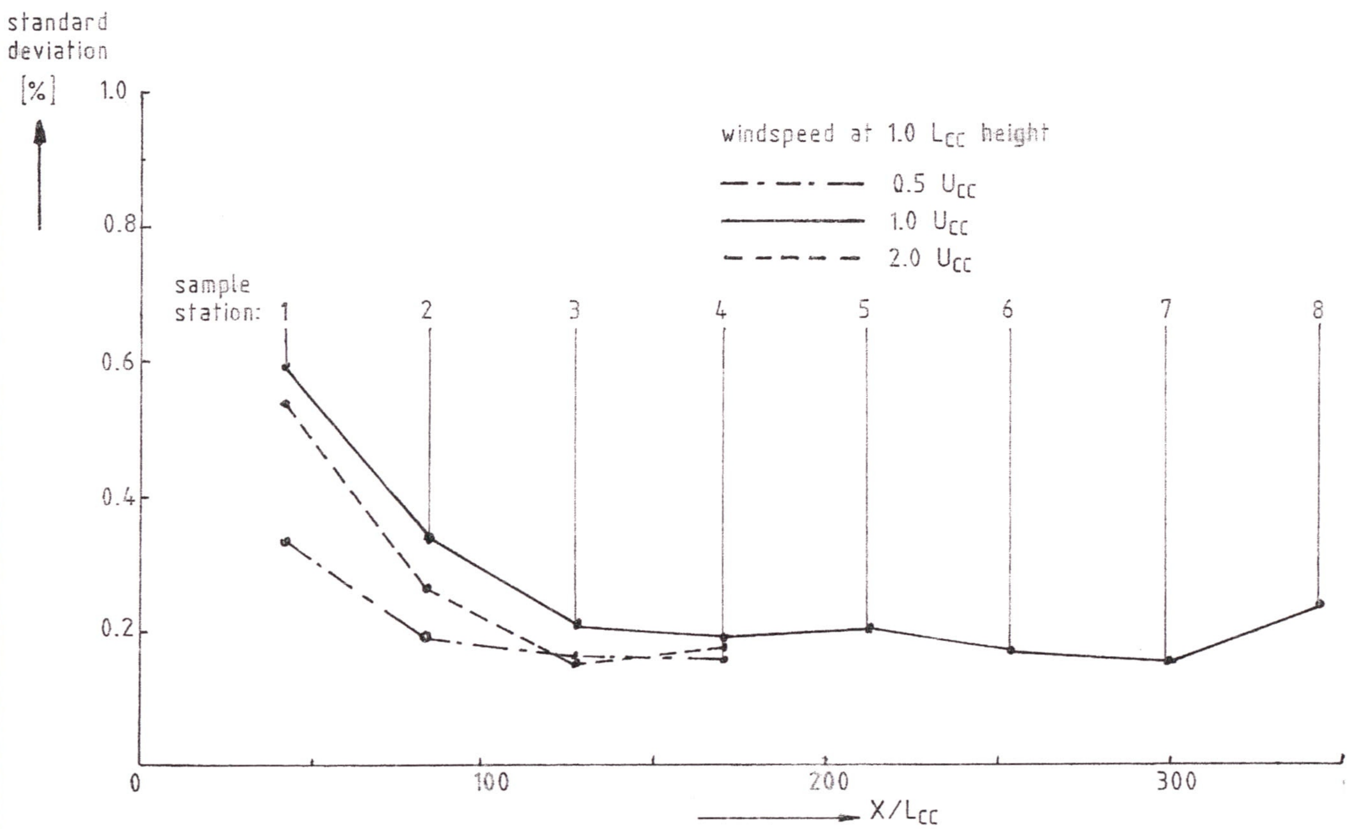

Standard deviation for the intercomparison continuous test and both additional tests.

MT-TNO
90-346
Fig.28